# CHEMOSENSITIZING EFFECT OF *STREPTOMYCES* CRUDE EXTRACT ON CISPLATIN-INDUCED APOPTOSIS IN HUMAN LUNG CANCER H460 CELLS

Miss Theint Myat Noe Paing -

จุฬาลงกรณ์มหาวิทยาลัย
CHULALONGKORN UNIVERSITY

A Thesis Submitted in Partial Fulfillment of the Requirements
for the Degree of Master of Science in Pharmaceutical Sciences and
Technology
Common Course
FACULTY OF PHARMACEUTICAL SCIENCES
Chulalongkorn University
Academic Year 2020
Copyright of Chulalongkorn University

ผลกระตุ้นความไวต่อยาของสารสกัดหยาบจากเชื้อสเตรปโตไมซีสต่อ
การตายแบบอะพอพโทซิสที่เหนี่ยวนำด้วยซิสพลาตินในเซลล์มะเร็งปอด
ของมนุษย์ชนิดเอช 460

น.ส.เธียท มยาท โน พาง -

จุฬาลงกรณ์มหาวิทยาลัย
CHULALONGKORN UNIVERSITY

วิทยานิพนธ์นี้เป็นส่วนหนึ่งของการศึกษาตามหลักสูตรปริญญาวิทยา
ศาสตรมหาบัณฑิต
สาขาวิชาเภสัชศาสตร์และเทคโนโลยี ไม่สังกัดภาควิชา/เทียบเท่า
คณะเภสัชศาสตร์ จุฬาลงกรณ์มหาวิทยาลัย
ปีการศึกษา 2563

| | |
|---|---|
| Thesis Title | CHEMOSENSITIZING EFFECT OF *STREPTOMYCES* CRUDE EXTRACT ON CISPLATIN-INDUCED APOPTOSIS IN HUMAN LUNG CANCER H460 CELLS |
| By | Miss Theint Myat Noe Paing - |
| Field of Study | Pharmaceutical Sciences and Technology |
| Thesis Advisor | PREEDAKORN CHUNHACHA, Ph.D. |
| Thesis Co Advisor | WONGSAKORN PHONGSOPITANUN, Ph.D. |

Accepted by the FACULTY OF PHARMACEUTICAL SCIENCES, Chulalongkorn University in Partial Fulfillment of the Requirement for the Master of Science

........................................... Dean of the FACULTY OF PHARMACEUTICAL SCIENCES
(Assistant Professor RUNGPETCH SAKULBUMRUNGSIL, Ph.D.)

THESIS COMMITTEE

........................................... Chairman
(Assistant Professor CHATCHAI CHAOTHAM, Ph.D.)

........................................... Thesis Advisor
(PREEDAKORN CHUNHACHA, Ph.D.)

........................................... Thesis Co-Advisor
(WONGSAKORN PHONGSOPITANUN, Ph.D.)

........................................... Examiner
(Assistant Professor CHAISAK CHANSRINIYOM, Ph.D.)

........................................... External Examiner
(Sudjit Luanpitpong, Ph.D.)

เธียท มยาท โน พาง - : ผลกระตุ้นความไวต่อยาของสารสกัดหยาบจากเชื้อสเตรปโตไมซีส ต่อการตายแบบอะพอพโทซิสที่เหนี่ยวนำด้วยซิสพลาตินในเซลล์มะเร็งปอดของมนุษย์ชนิด เอช 460  . ( CHEMOSENSITIZING EFFECT OF *STREPTOMYCES* CRUDE EXTRACT ON CISPLATIN-INDUCED APOPTOSIS IN HUMAN LUNG CANCER H460 CELLS) อ.ที่ปรึกษาหลัก : อ. ภก. ดร.ปรีดากร ชุณหะชา, อ.ที่ปรึกษา ร่วม : อ. ดร.วงศกร พงศ์โสภิตานันท์

ยาซิสพลาตินได้ถูกนำมาใช้เป็นการรักษาหลักในการรักษามะเร็งปอดด้วยยาเคมีบำบัด โดย ประสิทธิผลของยาถูกจำกัดด้วยการเกิดการดื้อต่อยาเคมีบำบัดของเซลล์มะเร็ง ซึ่งในการกระตุ้นให้มะเร็งเกิดมี ความไวต่อยาเคมีบำบัดเพิ่มขึ้นจากการใช้สารสกัดจากธรรมชาติก็อาจเป็นความพยายามอย่างหนึ่งในการรักษา มะเร็งที่ดื้อยาดังกล่าว ซึ่งในการศึกษานี้มีวัตถุประสงค์เพื่อศึกษาผลของสารสกัดจากเชื้อ *Streptomyces* sp. ใน บทบาทการเป็นสารกระตุ้นความไวต่อยาเคมีบำบัด ในการศึกษานี้ ได้ทำการศึกษา *Streptomyces* sp. ที่แยกได้ จากดินบริเวณป่าพรุในจังหวัดยะลาทั้งสิ้น 8 สายพันธุ์ โดยในจำนวนนี้พบว่า 3 สายพันธุ์มีความบริสุทธิ์จากการ วิเคราะห์ด้วย 16 rRNA sequencing จึงได้นำสายพันธุ์ที่มีความบริสุทธิ์สูงนี้ทำการศึกษาผลความเป็นพิษต่อ เซลล์มะเร็ง โดยพบว่าสารสกัดหยาบที่ได้จากสายพันธุ์ ST1-45 มีฤทธิ์ต้านมะเร็งปอดได้ดีโดยมีค่า $IC_{50} = 9.51$ µg/ml ดังนั้นจึงได้เลือกสารสกัดนี้เพื่อทำการศึกษาศักยภาพในการเป็นสารกระตุ้นความไวต่อยาเคมีบำบัดใน การศึกษาต่อมา ซึ่งในการศึกษาบทบาทในการเป็นสารกระตุ้นความไวต่อยาเคมีบำบัด ผู้วิจัยได้เลือกใช้สารสกัด หยาบของสายพันธุ์ ST1-45 ในช่วงความเข้มข้นที่ไม่เป็นพิษต่อเซลล์คือ 1.25 µg/ml ในการกระตุ้นความไวต่อ ยาซิสพลาตินซึ่งทดสอบในเซลล์มะเร็งปอดชนิดเอช-460 โดยจากผลการทดสอบการมีชีวิตของเซลล์พบว่าการ บ่มเซลล์ด้วยสารสกัดหยาบ ST1-45 ที่มีความเข้มข้น 1.25 µg/ml เป็นเวลา 1 ชั่วโมง แล้วบ่มเซลล์ต่อด้วยยา ซิสพลาติน พบว่าในกลุ่มที่มีการบ่มด้วยสารสกัด ST1-45 นั้นมีค่า $IC_{50} = 13.65$ µM ในขณะที่ยาซิสพลาติน เดี่ยวจะมีค่า $IC_{50} = 37.60$ µM ซึ่งบ่งชี้ว่าสาร ST1-45 อาจมีคุณสมบัติในการกระตุ้นความไวต่อยาซิสพลาติน ได้ การศึกษาได้ถูกยืนยันซ้ำด้วย Annexin V/PI staining โดยการอ่านผลจากเครื่อง Flow cytometry พบว่า การบ่มเซลล์ด้วย ST1-45 และซิสพลาตินทำให้การรอดชีวิตของเซลล์ลดลงอย่างมีนัยสำคัญทางสถิติและชนิด ของการตายของเซลล์เป็นแบบอะพอพโทซิส การศึกษาเกี่ยวกับกลไกการตายของเซลล์แบบอะพอพโทซิสนี้ได้ ศึกษาบทบาทของ Endoplasmic reticulum stress (ER stress) โดยติดตามระดับการแสดงออกของ IRE-1α, phospho-IRE-1α โดยพบว่าการตายของเซลล์เอช-460 ไม่มีความสัมพันธ์กับระดับของ IRE-1α, phospho-IRE-1α แต่อย่างใด นอกจากนี้ ผู้วิจัยได้ศึกษายืนยันจากการติดตามอัตราการเกิด *XBP-1* splicing ซึ่งผลก็ไม่มี การเปลี่ยนแปลงเช่นเดียวกับระดับของ phospho-IRE-1α จึงยืนยันได้ว่าการตายของเซลล์ไม่เกี่ยวข้องกับการ กระตุ้นอะพอพโทซิสผ่านกลไก ER stress แต่เป็นที่น่าสนใจที่พบอัตราการเกิด phospho-JNK มากขึ้นเมื่อเซลล์ ได้รับ ST1-45 ร่วมกับซิสพลาติน 10 mM แต่อย่างไรก็ดียังไม่มีความสัมพันธ์ที่ชัดเจนต่อการตายของเซลล์ และ การเปลี่ยนแปลงระดับของ ER stress จึงอาจเป็นไปได้ว่าการกระตุ้น phospho-JNK อาจมาจากวิถี upstream JNK signaling อื่นก็เป็นได้ ดังนั้นจึงควรมีการศึกษาเพิ่มเติมเกี่ยวกับกลไกการออกฤทธิ์ของ ST1-45 เพิ่มเติม ในอนาคต อย่างไรก็ดี ผลของ whole genome sequencing พบว่าสายพันธุ์ ST1-45 เป็น candidate ของ *Streptomyces* sp. สายพันธุ์ใหม่ซึ่งแยกได้จากประเทศไทย ความรู้ดังกล่าวนี้จึงเป็นองค์ประกอบสำคัญใน การศึกษาเพิ่มเติมเกี่ยวกับสารสำคัญที่ออกฤทธิ์ดังกล่าวและกลไกการออกฤทธิ์ที่ชัดเจน อันจะนำไปสู่การพัฒนา เป็นสารกระตุ้นความไวต่อยาซิสพลาตินได้ในอนาคต

| | |
|---|---|
| สาขาวิชา เภสัชศาสตร์และเทคโนโลยี | ลายมือชื่อนิสิต ................................................. |
| ปีการศึกษา 2563 | ลายมือชื่อ อ.ที่ปรึกษาหลัก ............................. |
| | ลายมือชื่อ อ.ที่ปรึกษาร่วม ............................... |

# # 6176125133 : MAJOR PHARMACEUTICAL SCIENCES AND TECHNOLOGY
KEYWORD:     Chemosensitizing effect ER stress Streptomyces Cisplatin

Theint Myat Noe Paing - : CHEMOSENSITIZING EFFECT OF *STREPTOMYCES* CRUDE EXTRACT ON CISPLATIN-INDUCED APOPTOSIS IN HUMAN LUNG CANCER H460 CELLS. Advisor: PREEDAKORN CHUNHACHA, Ph.D. Co-advisor: WONGSAKORN PHONGSOPITANUN, Ph.D.

Although cisplatin has been considered as a first-line chemotherapeutic drug for the treatment strategy of lung cancer, its curative efficacy is limited by the occurrence of drug resistance and adverse effects. The application of non-toxic natural products for sensitization of cancer cells to conventional drugs is a recent novel strategy for cancer management to tackle these problems. This study aims to investigate effective chemosensitizer produced by *Streptomyces* sp. on the growth inhibition of human H460 lung cancer cells. Herein, three of eight strains isolated from peat swamp forest, Yala Province, Thailand which showed good purity analyzed by 16S rRNA sequencing were screened for cytotoxic activity. Among these, crude extract ST1-45 with the highest anticancer activity ($IC_{50}$ = 9.51 µg/mL) was selected for further investigations. The optimal non-toxic dose of ST1-45 (1.25 µg/mL) was used to examine the sensitization effect on cisplatin-induced apoptosis in H460 cells. The viability assay suggested that the pretreatment of 1.25 ug/ml of ST1-45 significantly reduced IC50 of cisplatin from 37.60 µM to 13.65 µM. Therefore, this study revealed that non-toxic dose of ST1-45 can be used to sensitize H460 cells to cisplatin treatment. The findings from the annexin V/PI costaining by flow cytometry revealed that the induction of cell death by cotreatment with ST1-45 and cisplatin was due to apoptosis. The results of RT-PC analysis and western bot analysis showed that the underlying apoptotic mechanism of sensitization effect did not depend on IRE1 α-mediated ER stress pathway since IRE1 α mediated *XBP-1* splicing ratio which indicates mild ER stress condition did not change after treatment with ST1-45. Moreover, protein expression level of the ER stress marker pIRE1 α which is an upstream signaling molecule of *XBP-1* splicing and JNK activation did not alter in both treatment groups compared to control. Surprisingly, upregulation of pJNK protein was found in the cells treated only with ST1-45 and a combination of ST1-45 with cisplatin at 10 µM while there was no difference in total JNK protein. So, other upstream signaling pathways for example AMPK pathway could be one of the contributors that induce JNK activation. Therefore, Further studies are required to clarify the exact molecular mechanism of chemosensitization effect of ST1-45 on cisplatin-induced apoptosis. Lastly, strain identification of promising crude extract ST1-45 by whole genome sequence analysis proved that the strain ST1-45 could represent the candidate of novel species. The novel findings in this study highlight further to investigate major constituents in ST1-45 and subsequently evaluate the therapeutic effects of pure compound in cancer management.

| | | |
|---|---|---|
| Field of Study: | Pharmaceutical Sciences and Technology | Student's Signature ............................... |
| Academic Year: | 2020 | Advisor's Signature .............................. |
| | | Co-advisor's Signature ......................... |

# ACKNOWLEDGEMENTS

for their undivided support, sacrifices and their love that raised me again when I got weary; without whom I would be unable to complete my project.

Last but not the least, special thanks must go to my colleagues for loved, supported, encouraged, entertained, and helped me get through this agonizing period in the most positive way.

Theint Myat Noe Paing  -

# TABLE OF CONTENTS

**Page**

# LIST OF TABLES

จุฬาลงกรณ์มหาวิทยาลัย
CHULALONGKORN UNIVERSITY

**LIST OF FIGURES**

# LIST OF ABBREVIATIONS

| | | |
|---|---|---|
| ANOVA | = | analysis of variance |
| ASK1 | = | apoptosis signal-regulating kinase |
| ATCC | = | American Type Culture Collection |
| ATF 4 | = | activating transcription factor 4 |
| ATF 6 | = | activating transcription factor 6 |
| Bak | = | Bcl-2 homologous antagonist/killer |
| Bax | = | Bcl-2 associated X protein |
| BCA | = | bicinchoninic acid assay |
| Bcl-2 | = | B-cell lymphoma 2 |
| Bcl-xL | = | B-cell lymphoma-extra-large |
| BIM | = | Bcl-2-interacting mediator of cell death |
| $^{\circ}C$ | = | degree Celsius |
| $CaCO_3$ | = | calcium carbonate |
| CHOP | = | C/EBP homologous protein |
| $CO_2$ | = | carbon dioxide |
| DMEM | = | Dulbecco's modified eagle medium |
| DMSO | = | dimethyl sulfoxide |

| | | |
|---|---|---|
| DNA | = | deoxyribonucleic acid |
| dNTP | = | deoxy nucleotide triphosphate |
| DTT | = | dithiothreitol |
| EDTA | = | ethylenediaminetetraacetic acid |
| eIF2 α | = | eukaryotic translation initiation factor 2 alpha |
| ER | = | endoplasmic reticulum |
| ERAD | = | ER-associated degradation |
| EtOAc | = | ethyl acetate |
| FBS | = | fetal bovine serum |
| GADD34 | = | DNA-damage-inducible protein 34 |
| g/L | = | gram per liter |
| GRP 78 | = | glucose related protein 1 |
| h | = | hour, hours |
| $IC_{50}$ | = | inhibition concentration 50 |
| IRE 1α | = | inositol-requiring protein 1 alpha |
| ISP | = | International *Streptomyces* Project |
| JNK | = | JUN N-terminal kinase |
| MAPK | = | mitogen-activated protein kinase |

| | | |
|---|---|---|
| MgCl$_2$ | = | magnesium chloride |
| mL | = | milliliter |
| mM | = | millimolar |
| min | = | minute, minutes |
| MTT | = | 3-(4,5-Dimethylthiazol-2-yl)-2,5- diphenyl-tetrazoliumbromide |
| µg/mL | = | microgram per milliliter |
| µL | = | microliter |
| µM | = | micro molar |
| mmol/L | = | milimole per liter |
| NSCLC | = | non-small cell lung cancer |
| PBS | = | phosphate buffer saline |
| PCR | = | polymerase chain reaction |
| PDI | = | protein disulfide isomerase |
| % | = | percentage |
| PERK | = | protein kinase RNA-like ER kinase |
| pIRE 1α | = | phosphorylated inositol-requiring protein 1 alpha |
| pJNK | = | phosphorylated JUN N-terminal kinase |

| PI | = | propidium iodide |
| PVDF | = | polyvinylidene difluoride |
| RIPA | = | radioimmunoprecipitation assay buffer |
| RNA | = | ribonucleic acid |
| rpm | = | revolution per minute |
| RPMI | = | Roswell Park Memorial Institute |
| SCLC | = | small cell lung cancer |
| SDS-PAGE | = | sodium dodecyl sulfate-polyacrylamide gel electrophoresis |
| S.D | = | standard deviation |
| TE buffer | = | Tris-EDTA buffer |
| TLC | = | Thin Layer Chromatography |
| UPR | = | unfolded protein response |
| TRAF2 | = | tumor necrosis factor receptor-associated Factor 2 |
| U | = | unit |
| V | = | voltage |
| w/v | = | weight per volume |
| *XBP-1* | = | X-box binding protein |

# CHAPTER I

# INTRODUCTION

Cancers are characterized by abnormal cell proliferation with the potential to metastasize or promote invasion to other organs of the body (1). Even though new techniques for early detection of the disease's stages has been developed, cancer related death rates are still the second-highest rank of mortality around the world (2). Lung cancer is the highest rate of mortality and life-threatening disease among solid tumors including colon, prostate or breast cancer (3-5). Lung cancer is typically characterized into two main types namely small cell lung cancer (SCLC) and non-small cell lung cancer (NSCLC). SCLC which is a clinically aggressive type of tumor accounts for 15% of all lung cancer cases. In contrast, NSCLC which is diagnosed as 85% of lung cancers has three main subtypes: adenocarcinoma, squamous cell carcinoma, and large cell carcinoma (6-8). Chemotherapy is the primary standard of care in lung cancer treatment. However, concomitant adverse effects and resistance to current chemotherapeutic drugs has led to the search for new compounds or chemosensitizing agents that can increase the efficacy of standard chemotherapy. Several kinds of agents targeting on different pathways have been used for therapeutic treatment of lung cancer. One of the target is the ER stress pathway or UPR which is a critical role in survival and death of lung cancer (9).

During tumorigenesis, acute demand of protein biosynthesis requires for various cellular functions such as tumor migration, proliferation, often driven by oncogenic stimulation. The tumor microenvironment might also provide limited conditions of tumor growth and development. For this reason, cancer cells need to adapt to such a

selectable surrounding with hypoxia, pH variation and insufficient nutrient supply that can cause cellular stress (10-12). During such a stress state, abnormally folded proteins are accumulated inside endoplasmic reticulum (ER) lumen which is the main organelle for protein folding and biosynthesis (13). All these conditions can disrupt correct protein folding, eventually contributing to the accumulation of misfolded or unfolded proteins, creating a condition called ER stress (14). However, the cell has elaborated an evolutionary mechanism to detect these changes and restore homeostasis by activating signal transducing pathways, termed as Unfolded Protein Response (UPR) (13).

Three major sensors, located in transmembrane of ER, which are IRE1 α, PERK, and ATF 6 can monitor the unfolded or misfolded proteins and activate different interconnected downstream signaling cascades to influence the life–death decision. During initial stage of ER stress, the UPR system attempts to reestablish normal ER function by stimulating cellular adaptive process to reduce ER load and help in recovery. However, in the event of the failure of this adaptive process due to severe and prolonged stress, UPR triggers a cell death pathway, generally via intrinsic apoptotic cell death which is mainly mediated by PERK and IRE1 signaling (14). As a result, under extremely high level of ER stress conditions, UPR transforms the cell fate from pro-survival to pro-death (14). IRE1 which is the most prominent and evolutionary arm of UPR arbitrates ying and yang of cellular fate in objectionable conditions. IRE1 has dual functions which are kinase and endonuclease activity. Under mild ER stress condition, activated IRE1 splices *XBP-1* mRNA into mature form *XBP-1s* which mainly has a protective role by initiating a series of genes

involving in restoration of protein folding, whereas severe and prolonged ER stress stimulate IRE1 kinase activity, which increase JNK phosphorylation linking to apoptosis (15). Although ER stress is primarily a pro-survival adaptive response against various kinds of cellular insults, ER stress-mediated UPR switches from adaptation to destruction in case of unmitigated ER stress (14). Several studies described that inducing prolonged and sustained ER stress which can switch from pro-adaptive to pro-apoptotic mechanism offers a promising therapeutic strategy in the management of cancer.

First-line therapeutic options for the treatment strategy of all types of lung cancer comprise surgery and chemotherapy (16). Cisplatin is one of the most used and effective chemotherapeutic for lung cancer treatment. However, its application is limited due to deleterious effects and drug resistance throughout the treatment (17, 18). It is generally considered as cytotoxic that targets on damaging DNA of cancer cells resulting in inhibition of DNA replication, subsequently triggering apoptosis. Besides, it was currently revealed that cisplatin may trigger ER stress and non-nucleus-dependent apoptotic signal activation (19-21). Ye Xu and his colleagues were previously described the modulation of survival and death induction through ER stress signaling pathway during the course of cisplatin treatment in cancer cells. In accordance with this knowledge, several researchers are currently attempting at investigating natural antitumor or chemosensitizing compounds to enhance chemotherapeutic efficacy or reduce the adverse effects of cisplatin by deciphering the complex network of ER stress. This strategy may establish a novel approach in the regimen of lung cancer treatment (22).

In the background of drug discovery and development, compounds originated from the natural sources emerge as the promising strategy for cancer treatment in consideration of the selective cytotoxic activity on tumor cells other than normal cells. Moreover, they could also behave as potent chemosensitizers in combination with conventional chemotherapeutic drugs. In addition to the fact that they can enhance drug efficacy at lower dose levels, thus hampering dosage toxicity and drug resistance. Extracts form natural products; especially microbial origins have served as an infinite source of diverse molecules in many drug discovery efforts and let to the isolation of several important drugs. From variety of microorganisms, *Streptomyces* spp. which belongs to the group actinomycetes, are prominent microbial sources for production of vast number of novel and beneficial bioactive compounds (23). The exploration of novel *Streptomyces* species is particularly exciting since *Streptomyces* are highly likely to be producers of valuable secondary metabolites with interesting diverse biological activities. Notably, *Streptomyces* are prolific source of many clinically important drugs, including anticancer agents such as doxorubicin and bleomycin (24-27).

Since UPR provide a dual role in cancer progression, natural compounds contribute to cell death by inhibiting the adaptive UPR or by inducing sustained and severe ER stress (28). As a result of this beneficial effect, many researchers have been trying to explore the interplay between natural compounds and anticancer properties through ER stress mechanism in *vitro* and *vivo* (29-31). There are some examples of natural anticancer agents via modulation of ER stress. Tunicamycin, a nucleotide antibiotic produced by *Streptomyces lysosuperficus* can promote apoptosis of A549

NSCLCs through CHOP activation-mediated endoplasmic reticulum stress (32). Another example of tunicamycin which is a well-known ER stress inducer can enhance the antitumor effect of cisplatin in A549 human non-small cell lung cancer in *vitro* experiment by upregulation of GRP78 and JNK proteins (33). Considering this information, targeting apoptotic arm of UPR pathway by facilitating ER stress above a certain threshold in cell that already have a high dependency on UPR is a valid target for the development of new therapeutic approach in treatment of cancer. Therefore, the main objectives of this study are

1. To isolate the soil actinomycetes and investigate the anticancer activity of crude extracts in human H460 lung cancer cells.

2. To evaluate the chemosensitizing effect of extracts from *Streptomyces* sp. on cisplatin-induced apoptosis in human H460 lung cancer cells.

3. To identify the selected *Streptomyces* sp. by 16S rRNA gene sequence and whole genome sequence analysis.

First, we assume that our crude extract ST1-45 might induce UPR transducer IRE1 α mediated *XBP-1* splicing and consequently stimulate JNK activated apoptotic pathway in combined treatment with cisplatin. Unfortunately, our recent study revealed that IRE1 α-mediated ER stress pathway did not correlate with the underlying mechanism of sensitizing effect of ST1-45 on cisplatin-induced apoptosis. However, surprisingly, we discovered that expression level of phosphorylated JNK protein was upregulated in the treatment with ST1-45 alone and cotreatment with cisplatin. Therefore, apoptotic mechanism of chemosensitization effect might be due to other upstream signaling pathways that contribute to JNK activation.

# CHAPTER II

# LITERATURE REVIEW

## 1.Lung Cancer

Lung cancer is the life-threatening and top-ranking of cancer-related deaths in both men and women [44]. Its mortality rate exceeds that of the three most common types of cancers (colon, breast, and pancreatic). According to the statistical data estimation from the American Cancer Society, lung cancer is the most often diagnosed malignancy (2.3 million in total new incidence cases, 1.2 million in male, 1.1 million in female) per 100,000 person-years worldwide in 2019. Furthermore, lung cancer ranked first and the estimated 1.6 million deaths from lung cancer have been reported in 2019 (0.7 million deaths in men and 0.6 million deaths in women). The typical causes of lung cancers include tobacco smoking, exposure to secondhand smoke, air pollutants (e.g. PM2.5), family history of malignancy and occupational exposure to carcinogens [45, 46]. Lung cancer was traditionally categorized into two primary groups which are small versus non-small cell type, based on distinguishing of the histopathologic features and immunohistochemical markers [47]. The three main subtypes of NSCLC are adenocarcinoma, squamous-cell carcinoma, and large-cell carcinoma [48]. Adenocarcinoma which figures out almost 40% of lung cancers is derived from peripheral lung tissue and is tightly linked with smoking [43]. The causes of squamous-cell carcinoma are about 30% of lung cancers which typically happen close to large airways. Approximately 9% of lung cancers are large-cell carcinoma.

## 1.1.Treatment strategies for lung cancer

The strategies for lung cancer treatment are chemotherapy, surgery, radiotherapy, and immunotherapy. Surgery is the most effective, and cornerstone therapy for the patient with early-stage lung cancer (34). However, for the advanced stage of lung cancer, combination chemotherapy is considered the front line strategy and standard of care for this type of cancer (35). The several kinds of chemotherapeutic agents are used for the treatment of lung cancer. Among them, platinum-based agents (e.g. cisplatin and carboplatin) are the most effective and greatest promising chemotherapeutic agents in the treatment of patients with NSCLC. These agents induce their killing effects on cancer cells by targeting cellular DNA and subsequently trigger apoptosis (36). Even though damaged DNA stimulates DNA repair mechanism in normal cells, platinum-based compounds mainly target cancer cells which is deficient in DNA repairing efficiency and then contributes to apoptosis (37, 38). Nonetheless, the occurrence of resistance to cisplatin and severe adverse effects are big problems and limit the usefulness of this compound in the treatment of lung cancer.

## 2.Mechanism of cisplatin-induced apoptosis via ER stress pathway

The major molecular mechanism of cisplatin (platinum cooperating compound) in anticancer activity is the formation of intra-stranded and inter-stranded crosslinks by binding of platinum to DNA. This DNA damaging effect arrests the cell cycle and instigate cell death in rapidly proliferating cells (39). Another researcher group was postulated that cisplatin could induce pro-apoptotic signaling through induction of ER stress by increasing cytosolic calcium concentration and calpain-

dependent stimulation of the ER-specific caspase-12 even in enucleated cells without relying on the fundamental DNA damaging effect (19, 40). Suppression of ER-specific caspase-12 with the anti-caspase-12 antibody significantly reduced cisplatin-induced cell death (41). Moreover, expression of ER stress marker (GRP78/ HSPA5) is upregulated and overexpressed pro-apoptotic signaling molecules CHOP or PDI after cisplatin treatment. These facts suggest that endoplasmic reticulum could be a non-nuclear dependent apoptotic mechanism of cisplatin (42, 43). Ye Xu, et al. has been reported that cisplatin induces ER stress dependent cell death through the activation of IRE1-JNK pathway in human cervical cancer Hela cells. In the same study, they also revealed that ER stress inducing agent (e.g. tunicamycin) augmented the cytotoxicity of cisplatin to Hela cells (44).

## 3.Endoplasmic Reticulum Stress (ER stress) or UPR pathway

Although chemotherapy and radiation therapy are the standard options for lung cancer treatment, the mortality rate is still high due to resistance to these therapies and severe side effects. Therefore, there is an urgent need for new chemotherapeutic agents with minimal toxic effects to improve clinical outcomes. Since UPR activation is a major controlling pathway in lung cancer (9), researchers have been emphasized on the targeting of UPR pathway for new anticancer strategies. The ER is the foremost and large part of the compartment in the secretory pathway of the cell and controls the regulation of calcium level, lipid biosynthesis, folding and quality control of proteins. Approximately 30% of proteins across ER (45-47) towards their final destinations inside and outside of the cell. Biosynthesis of these proteins takes place in the cytosolic portion of the ER and productive protein folding is

integrated by intricate molecular machines located in the ER including chaperones, quality control proteins, and foldase. Although these controlling mechanisms provide protein biosynthesis from their nascent form to ER exportable type, some proteins are not folded properly and decline the criteria of a quality control system (48). These abnormal proteins are subjected to ER-associated degradation (ERAD) system which destroys them in cytoplasm by ubiquitinylation and proteasomal degradation (49). When ER encounters an important protein folding demand, the capacity of folding and degradation is delayed or ER capability of handling protein biosynthesis is overloaded, these conditions lead to an assembly of malfunctional proteins inside the ER lumen. This situation is called ER stress Response or UPR that attempts at (i) restricting unfolded proteins assembling in the ER by attenuating protein translation transiently; (ii) enhancing ER folding capacity (iii) increasing protein clearance from the ER by promoting its degradation capacity.

If ER stress still persists, UPR tends to trigger apoptosis (10). Activation of UPR is associated with the various pathological processes, including cancer (50). Due to the rapid expansion of malignant neoplasm, cancer cells are faced with nutrients deprivation, insufficient vascularization, and low oxygen supply. Under these condition, ER stress-related proteins including glucose-regulated protein 78 (GRP78), activating transcription factor 6 (ATF6), inositol-requiring protein 1(IRE1), protein kinase RNA-like ER kinase (PERK) are upregulated in cancer cells (51-53). Cancer cells initiate UPR to balance proteostasis system as an adaptive pathway for survival in response to a mild state of ER stress. Upon ER stress condition, GRP78 originally binds to the luminal domain of three ER transducer sensors to detect assembly of

misfolded proteins and maintain ER homeostasis (54). However, when ER stress is prolonged to the extent that UPR fails to cope with unfolded proteins, UPR is subjected to be turned into apoptotic machineries by transducing apoptotic downstream of UPR (55).
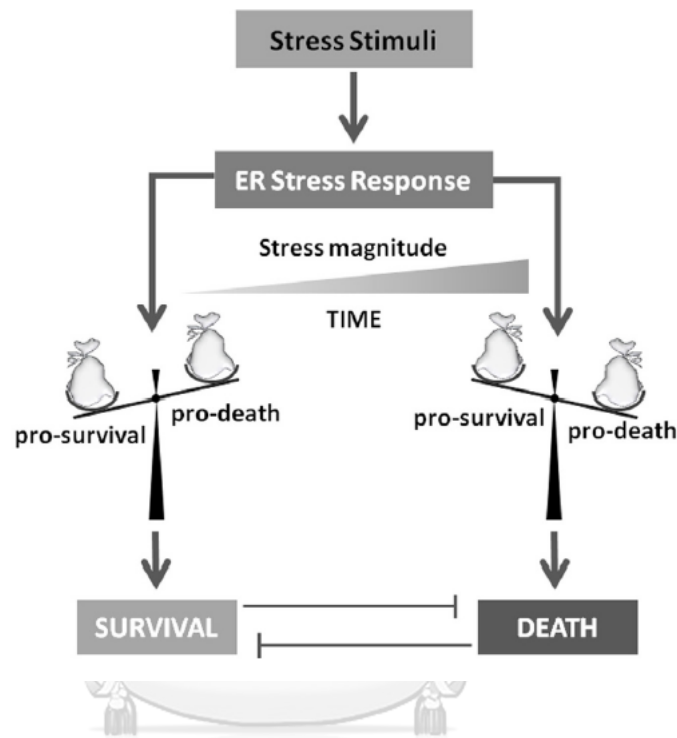


**Figure 1** To die or not to die (56).

## 3.1.Downstream signaling pathways of UPR

The three main types of mammalian UPR sensors are ATF6 (57), IRE1 α (58) and PERK (59) Fig.2.(60) , which are leading to decrease abnormally folded proteins, by attenuating de novo protein synthesis on the cytosolic part of the ER and by enhancing protein folding and clearance in the ER. The activation of these three sensors is managed by the ER-resident chaperone molecule called GRP78. Under normal conditions, GRP78 constitutively binds with the luminal sides of the sensors through the noncanonical binding, thereby inhibiting their activation (46, 61). In the

case of the assembly of misfolded proteins, GRP78 dissociates from the sensors through mechanism depending on its substrate binding domain (62). This trigger IRE1 α oligomerization and autophosphorylation (63) and simultaneous stimulation of the downstream signaling cascades. Besides, GRP78 dissociation from ATF6 α together with protein disulfide isomerase (PDI)-mediated disulfide bond modification (64) augment ATF 6 α export to the Golgi complex (65).

### 3.1.1. IRE1 Pathway

IRE1 which is the most evolutionarily conserved arm of the UPR, activate different processes, both physiological and pathological such as those inducing ERAD (66), lipid synthesis (67) and protein secretion (68). IRE1 is a type I protein receptor which contain an N-terminal ER luminal sensing domain and a cytosolic C-terminus domain enclosing both an endoribonuclease domain and a Ser/Thr kinase domain. There are two isoforms of IRE1 in human, IRE1 α and IRE1 β; the first one is expressed ubiquitously on the ER membranes, while the latter is found only on the epithelial cells of gastrointestinal tract (15). Upon the condition of ER stress, IRE1 α release from GRP78, dimerizes and autophosphorylates, converting into its active state. Activated IRE1 triggers its endonuclease activity which is responsible for X-box binding protein 1 (*XBP-1*) mRNA splicing. Spliced form of *XBP1* (*XBP-1*s) encodes for a stable transcription factor that targets genes involving in pro-survival responses (69). Moreover, active IRE1 α also interacts with tumor necrosis factor receptor-associated factor 2 (TRAF2) which leads to the increment of apoptosis signal-regulating kinase (ASK1) and JUN N-terminal kinase (JNK) and in turn, stimulate apoptosis.
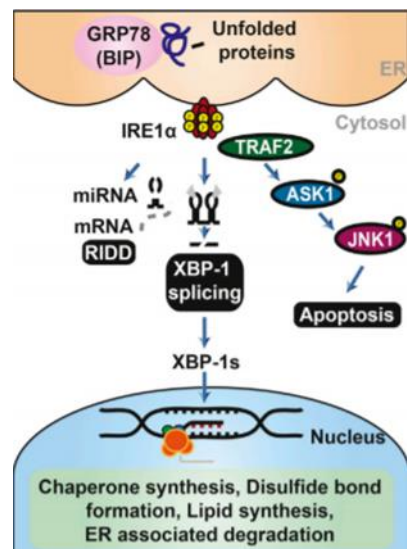
**Figure 2** The IRE1a axis (70).

### 3.1.2.PERK Pathway

PERK bind to GRP78 in its inactive form, however after dissociation from GRP78 in response to UPR triggering, it is activated by oligomerization and autophosphorylation (71). Activated form of PERK hinders mRNA translation and prevents the arrival of new proteins into the ER compartment which are mainly controlled by phosphorylation-mediated inactivation of the eukaryotic translation initiation factor 2 (eIF2 α). The eIF2 α phosphorylation prevents the recycling of eIF2 α in its active GTP-bound state that is required for synthesis of polypeptide chain, contributing to the attenuation of general protein translation. This process is critical for reducing the ER protein burden and to resolve ER stress (72). In the meantime, eIF2 α phosphorylation paradoxically regulates ATF4 expression, a member of the CCAAT/ enhancer binding protein family (C/EBP) family of transcription factors (73) . ATF4, in turn, controls the genes expression that are contained in the restoration of normal cellular homeostasis. C/EBP homologous protein (CHOP) and ATF4 upregulate the transcription of growth arrest and DNA-damage-inducible protein 34

(GADD34), which in turn renders the dephosphorylation of eIF2 alpha. If ER stress is irreversible, ATF4-CHOP activation can trigger the apoptotic pathway (74).
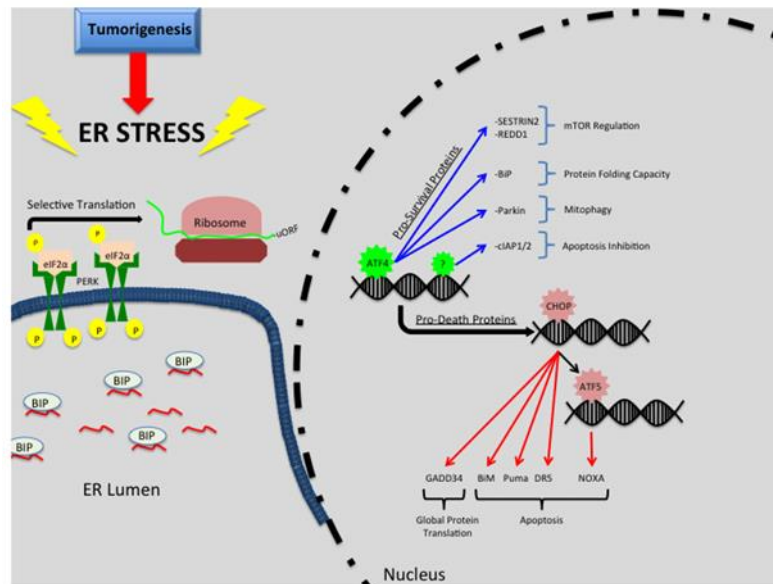


**Figure 3** Activation of unfolded protein response and downstream pro-survival and pro-death proteins (75).

### 3.1.3.ATF6 pathway

ER stress leads to ATF6 export from the ER to the Golgi apparatus where ATF6 alpha proteolytic cleavage by S1P and S2P proteases releasing an active membrane free form of ATF6f, which then translocate to the nucleus and activate the transcription of genes involving in protein folding and ERAD (46, 47, 76, 77).
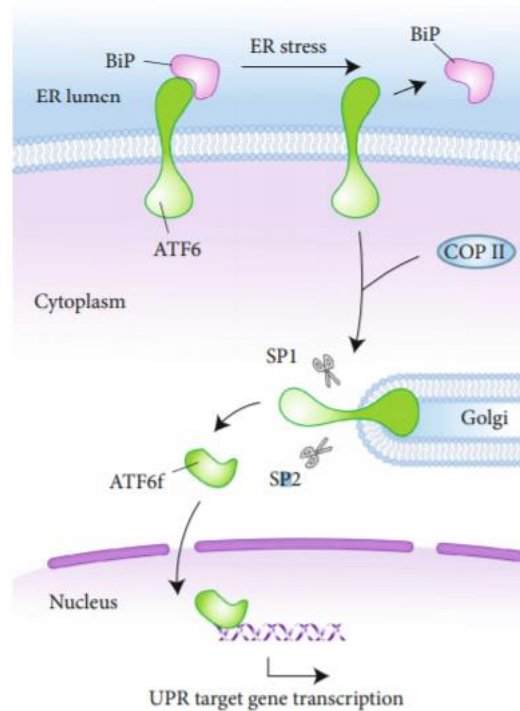
**Figure 4** The ATF6 axis of ER stress pathway (78).

**4.Anti-Cancer Strategy; Targeting IRE1α signaling pathway**

IRE1 α-*XBP-1* signaling pathway has been involved in cancer progression and *XBP-1* overexpression is observed in different types of cancers including breast cancer and hepatocellular carcinoma. Therefore, inhibition of IRE1 α-*XBP-1* could be a promising target for anticancer therapy (79). For example, deactivation of IRE1 α increase cytotoxic activity against human myeloma by reducing endonuclease activity in *vitro* and in *vivo* (80). Under severe and prolonged ER stress, IRE1 α activates the mitogen-activated protein (MAP) kinase (81). The IRE1 α binds to the TRAF2 and then triggers the stimulation of caspase-12 (82). Caspase-12 translocate from the ER to the cytosol, where it starts to cleave procaspase-9, in turn, activating the effector caspase, caspase-3 (83). IRE1 α/ TRAF2 stimulates ASK1, which consequently enhances activation and phosphorylation of JNK (71). Phosphorylated JNK activates

BIM, Bak, Bax and inhibits the Bcl-2 and Bcl-xL (84). This data indicate that the targeting IRE1-mediated apoptosis could also be a beneficial target for cancer therapy.

## 4.1. JNK signal transduction pathway

The stress activated protein kinase (SAPK)/c-Jun amino N-terminal kinase (JNKs) are the member of a larger group of serine/threonine (Ser/Thr) protein kinases known as the mitogen-activated protein kinase (MAPK) family (85). The mammalian JNKs are encoded by three distinct genes (*Jnk*1, *Jnk*2, and *Jnk*3) generated by alternative splicing, resulting in up to 10 different protein products which are varied in size (from 46 kDa to 55 kDa) (86). Two upstream MAPKKs which are mitogen-activated protein kinase 4 (MKK4) and MKK7 mediate the initiation of JNK activation. MKK7 and MKK4 preferentially phosphorylate JNK at threonine and tyrosine residues respectively, contributing to full activation of JNK (87, 88). The JNK signaling pathway involve in controlling of several cellular events such as cell development, proliferation, inflammation, and apoptosis. JNK can also behave as an anti-apoptotic or pro-apoptotic molecule depending on the circumstance. Numerous evidence show that MLM/JNK/c-Jun enhance apoptosis in cancer cells (89, 90). In addition, JNK can augment apoptosis by regulating p53 upregulated modulator of apoptosis (PUMA), which is a pro-apoptotic BH2-only protein through direct interaction with B-cell lymphoma 2 (Bcl-2) family (91-93).

## 5. Natural products for cancer therapy

Nature remains unlimited resources of novel bioactive molecules which are called natural products. Natural products are by-products and/or metabolites produced

by living organisms, such as microorganisms, plants, and animals (94, 95). The application of natural products from various sources is a boon to the emerging field of medicine in cancer therapy. Three quarter of antitumor compounds used in medicine are derived from natural origin and their related derivatives due to their low cost and availability. A significant number of natural products with antineoplastic activity have been produced by microorganisms. In particular, actinomycetes offer rich source of a wide variety of natural products with antitumor properties (96). Actinomycin D which was isolated from *Streptomyces antibioticus* is one of the earliest applications of a microbial product against stage I or stage II Wilm's tumor in children.

## 5.1.Characteristics of actinomycetes

The actinomycetes that are widely distributed in natural ecosystems around the world represent a ubiquitous group of microbes. As early as 1878, these organisms are originally recognized as 'Ray Fungi'. They are referred to as filamentous prokaryotes since they possess morphological forms such as filaments and conidia chains that occur in eukaryotic fungi and cell wall characteristics of prokaryotes. Earlier, they have been recognized as exotic group of organisms with affinities to both bacteria and fungi (97). However, their prokaryotic nature was confirmed by the determination of their fine structure and chemical composition (98, 99). Actinomycetes species are facultatively anaerobic, gram-positive bacteria showing a filamentous growth like fungi. These bacteria have been placed within the phylum *Actinobacteria*, order *Actinomycetales* which currently comprises 10 suborders, over 30 families and more than 160 genera. The structure of actinomycetes can be characterized by the formation of normally branching threads or rods and non-septate hyphae. The sporulating

mycelium may be straight or spiral-shaped in which the spores are cylindrical, spherical, or oval (100). Based on morphological characteristics, they are similar to fungi due to adaptation to same habitat otherwise their cell wall compositions resemble gram-positive bacteria. When the actinomycetes were grown on an agar-surface, they branch forming a network of hyphae growing both under-surface and on the surface of the agar. The under-surface hyphae are called substrate hyphae and on-the-surface hyphae are called aerial hyphae. Most actinomycetes are non-motile. The cell wall compositions of actinomycetes are greatly different among various groups and is of considerable taxonomic significance.

## 5.2.Distribution of actinomycetes

Actinomycetes have been found in all ecological niches such as soil, composts, water, extreme environments, marshy places. Among them, soil has an abundance population density. The actinomycetes in soil microflora rely on many factors which may be affected by soil type, pH, temperature, depth, water content, organic matter content, season, aeration, and agricultural contents. Most actinomycetes isolates behave as neutrophiles which are capable of growth at pH ranging from 5 to 9 with an optimal growth pH around 7. The pH, a major environmental factor, determines the activity and distribution of soil actinomycetes. Now, tropical peat swamp forests are recognized as important reservoirs of biodiversity (101) since it is home to an impressive diversity of species. Peat swamp forests, unique wetland ecosystems, are periodically flooded by fresh water from rainfall. Peatlands are identified as habitats where low oxygen conditions and waterlogged due to the accumulation of organic matter which is called peat. A high-

water table and wet conditions cause low oxygen diffusion rate into the sediment resulting in anoxic conditions. The peatlands are also specified as low pH systems as the accumulation of organic matters and anoxia contribute to the development of acidic conditions (102, 103). It was previously deduced that there was low bacterial diversity in such extreme environmental conditions. However, some researchers revealed that there were high diversity and complexity of genetic information of the bacteria by using metagenomic studies. Kanokratana, et al. reported that peat swamp forests in Thailand were an ecological niche of the microorganism constituting the most abundant microbial group.

## 5.3. Genetic analysis of actinomycetes

### 5.3.1. 16S rRNA gene sequence analysis

16S rRNA gene sequence is the most used housekeeping genetic marker to study bacterial taxonomy and phylogeny. The characteristic of the 16S rRNA gene, also called 16S ribosomal DNA which is encoded by the gene rrs is a polyribonucleotide of approximately 1500 nucleotides. Since this molecule is found in almost all bacteria, it is characterized as a powerful universal marker for bacterial classification. Moreover, its function has not changed over long periods and its structure is apparently maintained overtime, suggesting that change in random sequences are more accurate measure of time (evolution). Besides, 16S rRNA sequences provide sufficient variability to discriminate not only the most distant organisms but also the nearest levels such as strains, species, and varieties. The 16S rRNA gene consists of nine hypervariable or less-conversed regions which contribute the most useful information for taxonomic and phylogenetic studies. On the other

hand, the conserved regions are beneficial for designing universal primers which amplified the different hypervariable regions of the 16S rRNA genes in microorganisms (104). National Centre for Biotechnology Information (NCBI) which is the largest library of nucleotide database was used as reference libraries to compare 16S rRNA sequences of the bacteria for the determination of the species with maximum similarity. Sequence similarity > 99% to reference sequence is necessary for species level identification (105, 106).
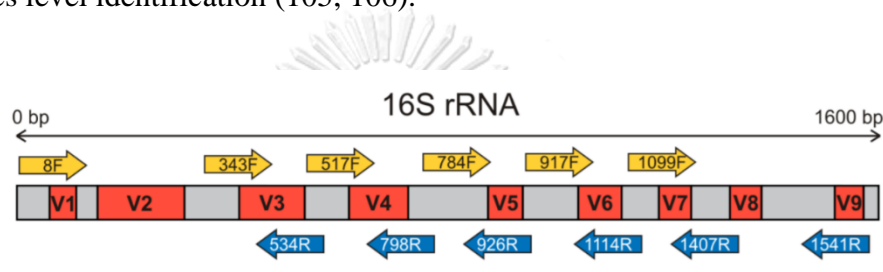


**Figure 5** 16S rRNA gene structure and possible primers (107)

### 5.3.2. Whole genome sequence analysis

Strain identification through whole genome sequencing (WGS) offers a far superior resolution compared to genetic marker-based techniques. The most basic level of bacterial information likely species and/or subtype can be characterized by using WGS that allow phylogenetic placement of a given sequence relative to an existing set of isolates (108). Beyond species characterization and identification, WGS provide a rich resource that can be exploited to predict secondary metabolites biosynthetic gene clusters (109).

### 5.4. Characteristics of *Streptomyces*

In 1943, Waksaman and Henrici introduced the genus *Streptomyces* which represent one of the largest taxonomic species of recognized actinomycetes. Genus

*Streptomyces* belongs to the phylum *Actinobacteria*, family *Streptomycetaceae* and order *Actinomycetales* within the class of *Actinobacteria*. They are characterized as aerobic, non-Acid-Fast, gram-positive bacteria (110). They are chemoorganotrophic, filamentous bacteria with high G+C content 69-78% (111). The diameter of filaments and spores are tiny usually 1 μm or less (112). The spores which are borne in wavy, straight, or helical chains are formed by the fragmentation of the filaments (113). The colonies are slow-growing and often have a soil-like odor due to the production of a volatile metabolite called geosmin (114). Firstly, the colonies are relatively smooth surfaced but in later they grow a weft of aerial mycelium with the appearance of powdery, floccose, powdery, or velvety (115). They also produce a various kind of pigments which are responsible for the coloration of the vegetative and aerial mycelia (116). *Streptomyces* sp. are mostly mesophile and grow in temperature of 10-37 ˚C and pH 6.5-8.0 (117, 118).

## 5.5. Life cycle of *Streptomyces*

The developmental cycle of *Streptomyces* starts with the germination of spore existing from its dormant state and subsequently forms germ tubes grown by tip elongation when a spore settles in a nutrient rich medium. The germ tubes grow out to extend and branch like a network of filaments which across and grow into the surface of an agar plate. This network is termed as the substrate mycelium (116). Differentiation of the mycelium in the center of the colony leads to the formation of new cell type, called the aerial hyphae. Robinow HC1-Giemsa method of nuclear staining has been applied to study the life cycle of a *Streptomyces* sp. and is demonstrated in the subsequent manner: (i) initial nuclear division phase; (ii) primary

mycelium; (iii) secondary mycelium; and (iv) spore formation (119). Apparently, the differentiation of morphological events in *Streptomyces* corresponds with the sensing of essential nutrients depletion. Meanwhile, *Streptomyces* begins to produce secondary metabolites when a stressful environment such as nutritional deficiencies encounter and this process is referred to physiological differentiation (120). Metabolic development is stimulated, and many beneficial secondary metabolites are produced to provide the survival of *Streptomyces* in stressful environments during the shifting phase from vegetative to aerial growth and sporulation (120-122).
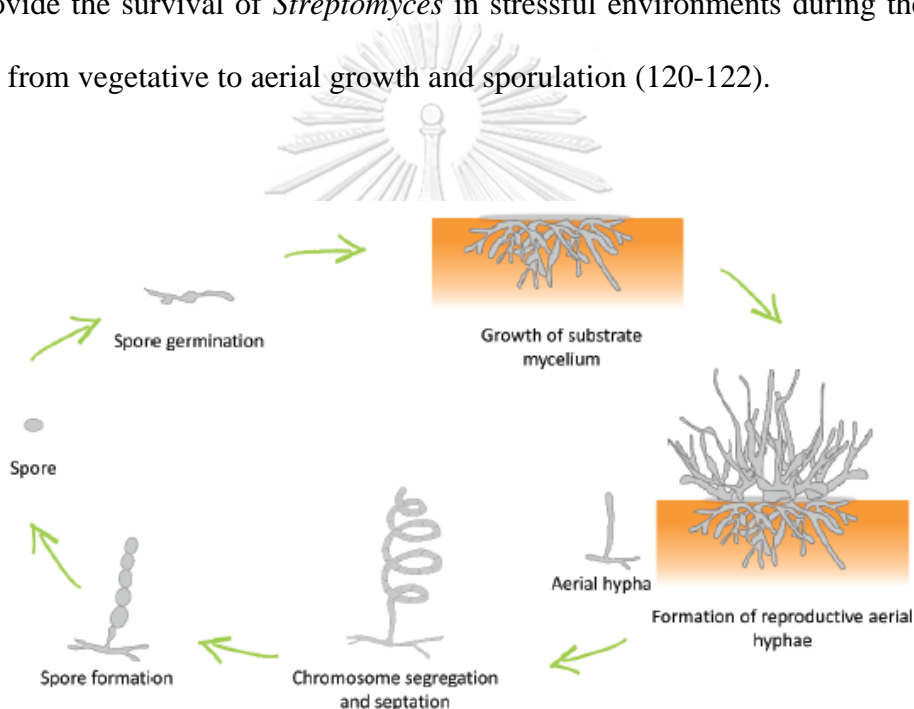


**Figure 6** Schematic representation of the life cycle of *Streptomyces*

**5.6.*Streptomyces* metabolites**

A primary metabolite which is typically found in many cells or organisms plays a vital role in physiological function of the organism such as normal growth, reproduction, and development (123). Unlike primary metabolites, secondary metabolites are not directly involved in the physiological process of the organism (124). Therefore, secondary metabolites are different from the primary metabolites in

four manner: i) they are not essential metabolites for organism's growth and development, ii) their production depend on the growth conditions for instance culture media type, iii) they are often possible to produce as groups of closely related molecules, and iv) they are often overproduced (125). Secondary metabolic pathway reactions are conducted using an individual enzyme or multienzyme complexes to obtain secondary metabolites. Intermediate or end products of primary metabolic pathways are obtained from their own systematic metabolic pathways for the synthesis of secondary metabolites. There are six known biosynthetic pathways: the peptide pathway, the polyketide synthase (PKS) pathway, the nonribosomal polypeptide synthase (NRPS) pathway, the hybrid (nonribosomal polyketide) synthetic pathway, the shikimate pathway, the β-lactam synthetic pathway, and the carbohydrate pathway. The genes that encode these synthetic pathway enzymes are generally present in chromosomal DNA mostly arranged in cluster formation (126). Most of the microorganisms synthesize secondary metabolites and their complex molecules at the stationary phase and lag phase of their growth. However, especially actinomycetes and *Streptomyces* can produce secondary metabolites at exponential, stationary, and death phase. The most significant characteristic of *Streptomyces* can produce secondary metabolites possessing antitumor, antibacterial, antifungal, and antiviral properties. Secondary metabolites produced by *Streptomyces* are doxorubicin as an anticancer agent (127), streptomycin as novel antibiotic drug and rapamycin as immunomodulatory agent (128).
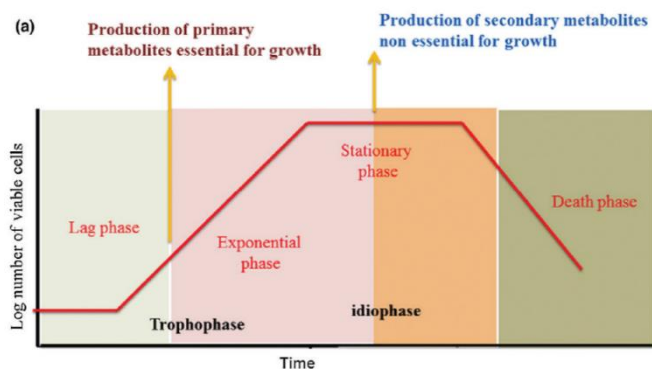
**Figure 7** Phases of bacterial growth and metabolite production

**5.7. Secondary metabolites with anticancer activity from *Streptomyces***

Actinomycin D which was isolated from *S. antibioticus* was the first natural metabolites applied in treatment of Wilms tumors in children. It binds DNA at the transcription initiation complex and prevent elongation process by RNA polymerase. But its application limited due to its many adverse effects (129). Other anticancer compounds obtained in 1960s during the biosynthesis process of *S. peuceticus* are daunorubicin, anthracyclines, and doxorubicin. Epirubicin, anthracycline compound which was approved by the FDA in 1999 is used in treatment of ovarian cancer, breast cancer, leukemia, and lung cancer. It possesses a better therapeutic profile than doxorubicin because of less side effects (130). Bleomycin, another antitumor compound produced by *S. verticillus* was approved by the FDA for clinical treatment in 1973. Streptozotocin, metabolite of *S. achromogenes*, was approved by the FDA in 1973 and shows selective toxicity against pancreatic beta cells (129, 131). Recently, new analogue of geldanamycin, 11-methoxy-17-formyl-17-demethoxy-18-O-21-O dihydrogen L danamycin, isolated from *S. hygroscopicus* possesses significant toxicity against human cancer cell lines (e.g. lung carcinoma COR-L23, breast cancer MCF-7, skin melanoma SK-MEL-2) (132). Resitoflavine, a quinone-related

antibiotic, isolated from a marine actinomycete, *S. chibaensis* shows cytotoxicity against gastric adenocarcinoma HMO2 and hepatic carcinoma HePG2 cell lines (133). Mansouramycins A-D, isoquinolinequinones isolated from *Streptomyces* sp. shows antitumor activity against lung cancer, prostate cancer, melanoma, and breast cancer (134, 135). Tartrolons which shows cytotoxicity against colon HT29, lung A549 and breast MDA-MB-231 was isolated from *Streptomyce*s sp.(136, 137). Carboxamycin produced by *Streptomyces* sp. shows antitumor activity against hepatocellular carcinoma (hepG2), gastric adenocarcinoma cell lines (AGS), and breast carcinoma MCF-7 (138, 139).

**5.8. Anticancer compounds from *Streptomyces* sp. targeting ER stress pathway**

Researchers have reported that some bioactive compounds extracted from the culture broth of *Streptomyces* sp. show anticancer activity through modulating ER stress pathway. Ilamcin E produced by *Streptomyces atratus* and *Streptomyces islandicus* attenuates UNBC cell growth and provoke apoptosis through activating the intrinsic apoptotic pathway via the ER stress/CHOP/Bcl-2 axis, providing a prospective therapeutic compound for breast cancer (140). Trierixin which is a new member of trieneansamycin antibiotic, isolated from *Streptomyces* sp. inhibit cancer progression by blocking ER stress-induced *XBP-1* activation (141). Tunicamycin which is commonly used as ER stress inducer extracted from the culture broth of *Streptomyces lysosuperficus* trigger cell death via ER stress-mediated CHOP activation in Human A549 NSCLC (32).

# CHAPTER III

# MATERIALS AND METHODS

## 1.Chemicals and Reagents

MTT, dimethylsulfoxide (DMSO), cisplatin, thapsigargin and STF083010 were obtained from Sigma-Aldrich Chemical (St. Louis, USA) and 0.25% trypsin-EDTA were purchased from Gibco (Gaitherburg,USA). Primary antibody of ER-stress related proteins (JNK, pJNK) and horseradish peroxidase (HRP)-labeled secondary antibody were procured from Cell Signaling Technology (Danver, USA). Phospho IRE1α was obtained from Abcam.

## 2.Cell Culture

Human H460 NSCLC cell line which was cultured in RPMI medium (Roswell Park Memorial Institute) and non-cancerous HaCat cell line which was cultured in Dulbecco's modified eagle medium (DMEM) were purchased from American Type Culture Collection (ATCC, Manassas, VA, USA). All the supplement reagents that are used in culture medium (10% fetal bovine serum FBS, 2 mM of L-glutamine and 100 units/mL of penicillin/streptomycin solution) were procured from Gibco (Gaithersburg, MA, USA). Both types of cell lines were maintained in culture plate with ultra-flat bottom surface to attach the cells with an optimum condition at 37˚C in the incubator, providing 5% $CO_2$ humidified atmosphere. 70-80 % confluence of the cells in the culture plate were used to proceed experiments.

## 3.Isolation of actinomycetes

The soil samples were collected from peat swamp forest at Yala province, Thailand. The collected soil samples were subjected to pretreatment with air-dried at

25 ˚C for 7 days. The air-dried sample was subjected to dried heat at 100˚C for 1 h. For phenol treatment, the air-dried soil samples were added in 1.5% phenol for 30 min. After that, soil samples were suspended in a basic lauryl sulfate solution. Serial dilutions of soil suspension were performed by the 10-fold serial dilution method. The aliquots (100 µL) of suspension of dilution were spread on surface of humic acid-vitamin agar medium and arginine vitamin agar medium, supplemented with cycloheximide 50 µg/mL and nalidixic acid 25 µg/mL and incubated for 30 days at 30 ˚C. The different colonies were picked up and streaked for further purification by streak plate technique on International *Streptomyces* Project (ISP) medium 2 and incubated for 14 days at 30 ˚C. They were also preserved by lyophilization using 10% w/v skim milk as a cryoprotectant solution for long-term storage.

**4.Fermentation and extraction from soil *Streptomyces* sp.**

A loop of spores of colonies was inoculated into 50 mL test tubes containing 10 mL of 301 seed medium that consist of 24 g/L starch, 1 g/L glucose, 3 g/L peptone, 3 g/L meat extract, 5 g/L yeast extract and 4 g/L $CaCO_3$ (adjusted to pH 7.0 before sterilization). Seed cultures were incubated on a rotary shaker (180 rpm) at 30 ˚C for 3 days. One percent of seed culture was transferred into 500 mL Erlenmeyer flask containing 200 mL of ISP2 production medium for 5 flasks. ISP2 production medium contains 4 g/L of Bacto-yeast extract (Difco), 1 g/L of Bacto-malt extract (Difco), 4 g/L of Bacto-dextrose (glucose) and pH of the medium was adjusted to 7 before sterilization. After that, the medium was autoclaved by using moist heat sterilization (121˚C for 15 min) before proceeding experiment. Finally, fermentation was carried out on a rotary shaker (200 rpm) at 27˚C for 7 days. One liter of culture

medium was extracted with the equal volume of ethyl acetate (EtOAc) for two times per one flask. The EtOAc layers were collected and evaporated to dryness by using a rotary evaporator. To completely remove residual solvent, crude extracts were placed in a vacuum desiccator overnight.

**5.Extraction of genomic DNA for 16S rRNA gene sequence analysis**

One loop of colonies was streaked on ISP2 agar plate and incubated for 3-5 days at room temperature. After incubation, one or two loops of bacterial colonies was put into the Eppendorf tube and added 300 µL of 100 mM TE buffer. Then 1 small spoonful of aluminum oxide was added into the tube and break the cells using micro multimixers for 90 sec. 300 µL of phenol: chloroform (1:1) was added into the tube, mixed for 5 minutes and centrifuged at 14,000 rpm for 15 minutes. The clear supernatant was transferred into a new tube. Then 1/10 volume of 3mM sodium acetate and 2 volumes of 95% cold ethanol were added and kept at -20˚C for 30 min. After that, centrifuged at 14,000 rpm for 15 min and the clear solution was removed, dried the DNA pellet. Firstly, the DNA pellet was washed with 70% ethanol, then washed again with 95% ethanol and dried the pellet for about 2 h. Finally, DNA pellet was dissolved in 30 µL of distilled water and measured the DNA content using nanodrop UV-Vis spectrophotometer (Thermo Scientific).

**6.Amplification of 16S rRNA gene**

The two primers, 20F (5'-GAGTTTGATCCTGGCTCAG-3') and 1530R (5'-GTTACCTTGTTACGACTT-3') were used for 16S rRNA gene amplification. The final volume (50 µL) of PCR mixture was contained 2 µL of each primer (10 pmol/µL), 1 µL of 10 mM dNTP, 5 µL of 10X *Taq* buffer, 2 µL of 50 mM MgCl2,

0.25 µL of *Taq* polymerase, 35.75 µL of distilled water and 5 µL of DNA template. The PCR conditions are 94°C for 3 min, followed by 29 repeated cycles containing 94°C for 1 min, 50°C for 2 min, 72°C for 2 min, and finally termination for 3 min at 72°C and 16°C forever. For the next step, the obtained PCR products were separated on 0.8% agarose gel containing 4 µL of red safe dye for 25 min with a voltage of 100V. The PCR band was checked with UV light. Following this step, PCR cleanup was performed using PCR purification kits (Geneaid). Lastly, the samples were sent for Macrogen; Seoul, Korea for sequencing of 16S rRNA gene using universal primers which are 27F (5'-AGAGTTTGATCMTGGCTCAG-3'), 518F (5'CCAGCAGCCGCGGTAATACG-3'), 800R (5'-TACCAGGGTATCTAATCC-3') and 1492R (5'-TACGGYTACCTTGTTACGACTT-3'). EzBioCloud database was applied for the identification of closest phylogenetic neighbors by BLAST search. Before construction of phylogenetic tree, verification, and the process of multiple-aligned with the selected sequences in 16S rRNA gene sequence must be performed manually. MEGA 7.0 software was applied for generation of phylogenetic tree using the neighbor-joining (NJ) methods. Kimura's two-parameter method was used in analysis of evolutionary distances among the stains for NJ tree. Support values of branches were evaluated using the bootstrap resampling method with 1,000 replications.

**7.Whole genome sequencing analysis**

Genomic DNA of strain ST1-45 was extracted using PureLink^TM Genomic DNA mini kit (Invitrogen). The genomic DNA was sequenced using the MiSeq sequencing system (Illumina). The whole-genome sequencing library of 250 bp was

prepared using QIAGEN FX kit (Qiagen, USA). Briefly, the genomic DNA was enzymatically fragmented and cleaned with magnetic beads. Next, the fragmented DNA was bind to the adaptor index. Cluster generation and paired end 2x250 nucleotide read sequencing were performed on Illumina MiSeq sequencer. The bioinformatics data of the genome was analyzed using PATRIC (142). The phylogenomic was constructed using TYGS web-based server (143). The calculation of average nucleotide identity (ANI) between the genome of strains was achieved with JspeciesWS (144). AntiSMASH software was applied for the determination of the biosynthetic gene cluster in the genome (145).

## 8.Cell viability assay

Human non-small cell lung cancer cell line (NCI-H460) (ATCC HTB-177 American Type Culture Collection) was incubated in complete RPMI-1640 medium with 5% $CO_2$ at 37˚C. Briefly, 100 $\mu$L of cell suspension with a density of $1 \times 10^5$ cell/well was seeded in 96 well plates and cultured for 24h. After that, culture medium was replaced with 100 $\mu$L medium containing various concentrations (ranging from 0.625 µg/mL to 160 µg/mL) of crude extracts from *Streptomyces* sp. for 24 h. After 24 h incubation, the supernatant was removed, washed with PBS and incubated with 100 µL of MTT solution (0.4 mg/mL to 0.5 mg/mL) for 4 h in the dark condition. The formazan crystals formed in the cells were dissolved with 100 $\mu$L of DMSO and measured at 570 nm using a microplate reader (Anthros, Durham, NC, USA). Cytotoxicity of each sample was expressed as an $IC_{50}$ value. The $IC_{50}$ value is the concentration of the test sample that causes 50% inhibition of cell growth averaged from three replicate experiments.

**9.Nuclear staining assay**

Costaining with Hoechst 33342 and propidium iodide (PI) are used to detect apoptotic and necrotic cell death. H460 cells were seeded at a density of $1\times10^5$ cells/well in 96 well plate for 24 h. Different concentrations of crude extract were treated on the cultured cells for 24 h. After 24 h treatment, the cells were stained for 30 min with concentration of 10 µM Hoechst and 5 µg/mL PI at 37˚C. The mechanism of cell death was examined under fluorescence microscope (Olympus IX51 with DP70).

**10.Isolation of RNA for *XBP-1* splicing assay**

After reaching nearly 70%-80% cell confluence, these cells were seeded into 6 well plate at a density of $3 \times 10^5$ cells/well for 24 h. After 24 h incubation, the culture medium was removed and treated with 1 mL of medium containing subtoxic dose of crude extracts from *Streptomyces* sp. for 24 h. The next step was harvesting the cells and then lyse the cell by using 300 µL of Trizol reagent. After adding the reagent, the cell lysate should be passed several times through a pipette to form a homogenous lysate. To ensure complete dissociation of nucleoprotein complex, the sample could stand for 5 min at room temperature before adding 60 µL of chloroform solution. The sample was covered tightly, shake vigorously for 15 sec, and allowed to stand for 2-3 min at the room temperature. The resulting mixture was centrifuged for 15 min at 12,000 x g and 4˚C. Following centrifugation, the aqueous phase was transferred to fresh tube and 150 µL of isopropanol was added to the tube and leave at room temperature for 10 min. Then the mixture was centrifuged for 10 min at 12,000 $\times$ g and 4˚C. The RNA precipitate was formed a pellet on the side and bottom of the tube.

And then the supernatant was removed and washed RNA pellet by adding 300 µL of 75% ethanol. Following this step, vortex the sample briefly and then centrifuge at 7,500 x g for 5 min at 4°C.The supernatant was removed by aspiration and air-dry RNA pellet for 5-10 min at room temperature. Finally, RNA pellet was solubilized in 20 µL of nuclease free water and then incubated in a water bath at 55-60°C for 10-15 min. The content of RNA yield was determined by using nanodrop UV-Vis spectrophotometer (Thermo Scientific).

**11.cDNA synthesis by RT PCR method**

Total RNA samples were reverse transcribed with the Invitrogen SuperScript III reverse transcriptase according to manufacturer's instruction. 200 ng of total RNA was added to a nuclease free PCR tube containing 1µL of 10 mM dNTP and 1 µL of 5 µM oligo dT. Nuclease free water was added into the tube to make up the final volume of 10 µL. The mixture was briefly centrifuged, heated to 65°C for 5 min in a heat block and cool to 4°C for at least 1 min. After that, the RT reaction mixture that comprise 2 µL 10x RT buffer, 4 µL of 25 mM MgCl$_2$, 2 µL 0.1 M DTT, 1 µL of RNaseOUT (40U/µL) and 1 µL of (200 U/µL) Super Script III reverse transcriptase was added to the tube containing mixture of RNA template, OligodT primer and dNTP mixture. The mixture solution was briefly centrifuged and heated to 50°C for 50 min. At the final step, the reaction was inactivated by heating at 85°C for 5 min. Hereafter, 1 µL of RNase H was added to each tube and incubated the tubes for 20 min at 37°C. The content of single stranded cDNA yield was determined by using nanodrop UV-Vis spectrophotometer (Thermo Scientific).

**12. PCR amplification and *PstI* digestion**

PCR products were synthesized from single stranded cDNA by PCR in a total volume of 20 µL containing 50 µM of *XPB1*-forward primer (5'-AAACAGAGTAGC TCAGACTGC-3') and *XBP-1* reverse primer (5'-TCCTTCTGGGTAGACCTCTGGG AG-3'), 10 mM of dNTP (NEB), 5 U/µL of NEB *Taq* Polymerase, 10X Standard *Taq* buffer, 5 M Betaine and nuclease free water. *XBP-1* double-stranded cDNA was synthesized under the following thermal cycling conditions: 94°C 2 min, 94°C 30 seconds 34 cycles, 58°C 30 seconds, 72°C 1 min, 72°C 3 min. Then, PCR products were digested with *PstI* digestion reaction containing 1 µg PCR product, 1.5 µL *PstI-HF*, 2 µL NEBuffer 4, water (up to 20 µL) at 37°C for 3 h followed by heat inactivation at 80°C for 20 min. The digested fragments were run on 2% agarose gels for approximately 1 h with 130 voltage (V). Following this step, the gel was stained with 0.5 µg/mL of ethidium bromide for 2 min and destained with deionized water for the same time. At the final step, the bands were detected with Gel Doc XR+ system (Bio-Rad). The ImageJ software (Version 1.4.3.67) was used to identify band intensity.

**13. Chemosensitization and selective cytotoxicity assay**

MTT was used to reveal the chemosensitization and selective cytotoxic effect of crude extract isolated from *Streptomyces* sp. on cisplatin-induced apoptosis in H460 cells. The cells were seeded into $1\times10^5$ cell/well in 96 well plates and incubated for 24 h in incubator. Then the cells were pretreated with nontoxic dose (1.25 µg/mL) of crude extract for 1 h followed by the treatment of various concentrations of

cisplatin (2.5 µM to 40 µM) for 24 h. For selective anticancer activity, the crude extract ranging from 0.325 µg/mL to 5 µg/mL was treated on both cancerous H460 cells and non-cancerous HaCat cells for 24 h. After that, percentage of cell viability was measured by microplate reader (Anthros, Durham, NC, USA).

## 14. Apoptotic analysis by flow cytometry using annexin V-PI

To detect the pattern of programmed cell death (apoptotic or necrotic cell death), H460 cells were seeded at a density of $1.5 \times 10^5$ cell/mL for 24 h. After treated with cisplatin alone and combination of cisplatin and crude extract on human H460 lung cancer cells for 24 h, these cells were harvested, washed with PBS and suspended the cells in 90 µL of annexin V binding buffer. Next, these cells were stained with 5 µL of each FITC-conjugated Annexin V and PI and subjected to flow cytometer according to manufacturer's instructions (ImmunoTools, Germany). The cell's populations are divided into four groups: (i) living cells without apoptosis or necrosis (no red or green fluorescence), (ii) early apoptotic cells (positive green fluorescence and negative red fluorescence), (iii) late apoptotic cells exhibiting both green and red fluorescence, and (iv) necrotic cells showing only red fluorescence (146).

## 14. Western blot analysis

The cell lysates were collected after treatment with cisplatin and crude extracts and then total protein was extracted using cell lysis buffer (RIPA buffer from Thermo scientific, Rockford, USA) and protease inhibitor (cOmplete™ ULTRA Tablets, Mini,

*EASYpack* Protease Inhibitor Cocktail) for 30 min to 1 h on ice. The cell lysates were centrifuged at 10,000 rpm for 4°C for 15 min and collected the supernatant. Protein concentration of each sample was measured by BCA protein assay kit (Thermoscientific). Before loaded on SDS-PAGE gel, the protein content of each sample was normalized and heated at 95°C for 5 min in the water bath for denaturation. After this step, equal amount of proteins was loaded on SDS-PAGE and separated by electrophoresis with the voltage of 80V for 2 h using running buffer. After finishing this step, the proteins were transferred onto nitrocellulose membrane (Bio-Rad, Hercules, CA, USA) using semi-dry transfer method. The transferred membrane was blocked with 5% w/v skim milk in TBST for 1 h at room temperature followed by incubation of primary antibodies against pIRE1 α, JNK, and pJNK overnight at 4°C. Then, the membrane was washed with TBST for three times and further incubated with relevant secondary antibodies for 2 h at room temperature. Eventually, protein bands from each sample were visualized using chemiluminescent ECL assay kit (Clarity$^{TM}$ western ECL substrate, Biorad). Image J software was used for quantitative determination of protein expression levels.

## 15. Analytical thin layer chromatography Profile

The TLC profile of the crude extract was performed on silica gel 60F$_{254}$ pre coated aluminium plates (Merck) with the layer thickness 250 µm. The developing solvent system used was the ratio of chloroform and methanol (9:1). After running TLC, the plates were visualized under normal white light, UV light at 254 nm and 365 nm. Derivatization reagents such as anisaldehyde, Dragendorff's Reagent, ninhydrin,

iodine vapour, phosphomolybdic acid, 50% aqueous sulphuric acid, 10% alcoholic sulphuric acid were exposed to the TLC plate for the detection of compounds.

**16.Statistical analysis**

All the mean data ± standard deviation represent from the three or more independent experiments. Comparison of significant differences among groups were examined using analysis of variance (ANOVA), followed by Tukey's posthoc test. IBM SPSS statistics 22 program was used for data analysis. *P* value for statistical significance is considered at ≤ 0.05.

**Experimental design**

> Preparation of crude extracts from soil actinomycetes

> Examination on cytotoxic effect of crude extract in human H460 cells

> Selection of potential crude extract with potent anticancer activity for further experiments

> Evaluation of sensitizing effect on cisplatin-induced apoptosis in human H460 cells

Sensitization Assay

- ✓ MTT assay
- ✦ Cisplatin alone
- ✦ Combination of cisplatin and crude extract

- ✓ Flow cytometry analysis
- ✦ Cisplatin alone
- ✦ Combination of cisplatin and crude extract

Mechanism

- ✓ RT-PCR analysis (To investigate *XBP-1* splicing level)
- ✓ Western blot analysis (To detect ER stress-related proteins level) - pIRE1 α, JNK, pJNK

> Identification of isolated soil actinomycetes based on 16S rRNA gene sequence and whole genome sequence analysis

2.2 Research Framework



Unfolded protein

Hypoxia

pH change

Nutrient deprivation

**ER Stress**

UPR

ADAPTIVE

*XBP-1* Splicing

Cell survival

M
A
L
A
D
A
P
T
I
V
E

JNK

Apoptosis

# CHAPTER IV

# RESULTS

## 1.Isolation and screening of cytotoxic activity of *Streptomyces* crude extracts

From eight crude extracts isolated from soil actinomycetes in peat swamp forest of Yala Province, only three of them (ST1-45, ST1-64, and ST1-54) provided good purity and the remaining crude extracts showed contamination with other strains based on 16S rRNA gene sequence analysis. Therefore, crude extracts isolated from pure strain were selected for screening of cytotoxic effect. The extraction yeild of crude extracts (ST1-45, ST1-64, and ST1-54) are found to be 100 mg, 98.51 mg, and 105.30 mg respectively.

To assess the cytotoxicity of these crude extracts, human H460 cells were treated with various concentrations of crude extracts (ranging from 0 µg/mL to 160 µg/mL) for 24 h. After the indicated time point, the percentage of cell viability was evaluated by MTT assay. Among primary screening for cytotoxic activity of these extracts, significant dose-dependent inhibitory activity of ST1-45 was initiated at a low dose (2.5 µg/mL) with $IC_{50}$ value of 9.51 µg/mL whereas the remaining two extracts (ST1-64 and ST1-54) which are $IC_{50}$ values of 337.37 µg/mL and 171.52 µg/mL respectively were found to reduce cell viability only at higher concentrations. Therefore, ST1-45 with a highest cytotoxicity against H460 cells was selected for further investigations (Fig.8).

Furthermore, to determine whether the growth inhibitory activity of ST1-45 was correlated with apoptosis. After treatment with various concentrations of ST1-45

for 24 h, the morphological characteristics of apoptosis and necrotic cells have been examined by staining with blue fluorescence dye Hoechst 33342 together with red fluorescence dye propidium iodide. Changes in morphological characteristics were observed under fluorescence microscope. Increasing the number of bright blue fluorescence cells with chromatin condensation, DNA fragmentation and formation of blebs on cell surface were found in a dose-dependent manner. However, few numbers of necrotic cells with red fluorescence were only occurred at high concentrations. This may suggest that ST1-45 induce growth inhibition of H460 cells through apoptosis (Fig.9).

**(a)**
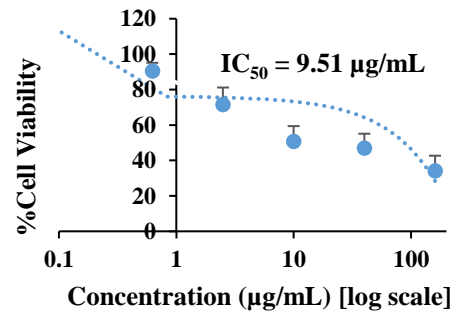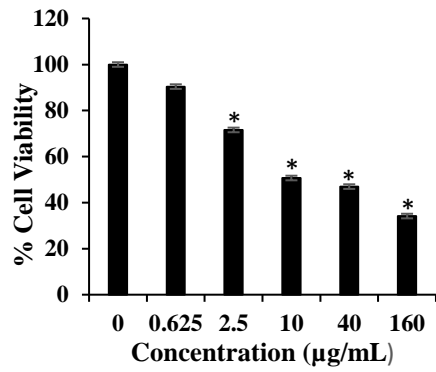


**(b)**
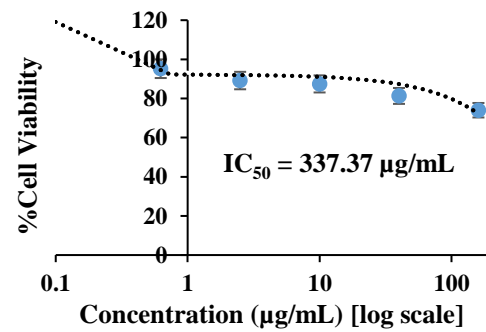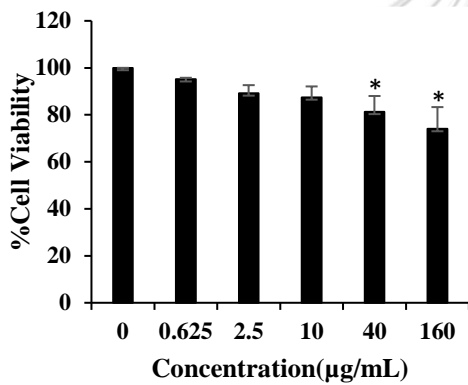


**(c)**
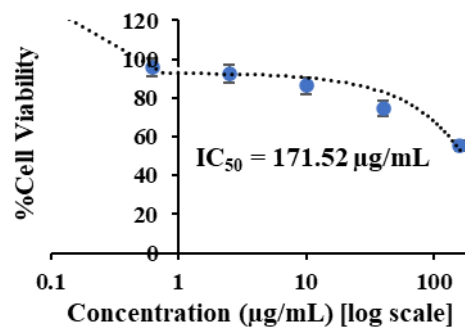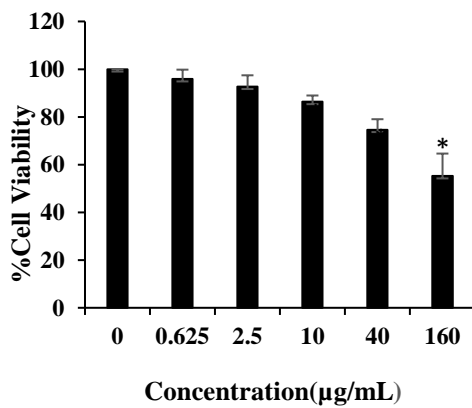
**Figure 8** Determination of cytotoxicity of *Streptomyces* crude extracts. (a) ST1-45 (b) ST1-64 (c) ST1-54. Values are means of the five independent experiments ± SD.*$P$ value ≤ 0.05 versus non-treated control group.
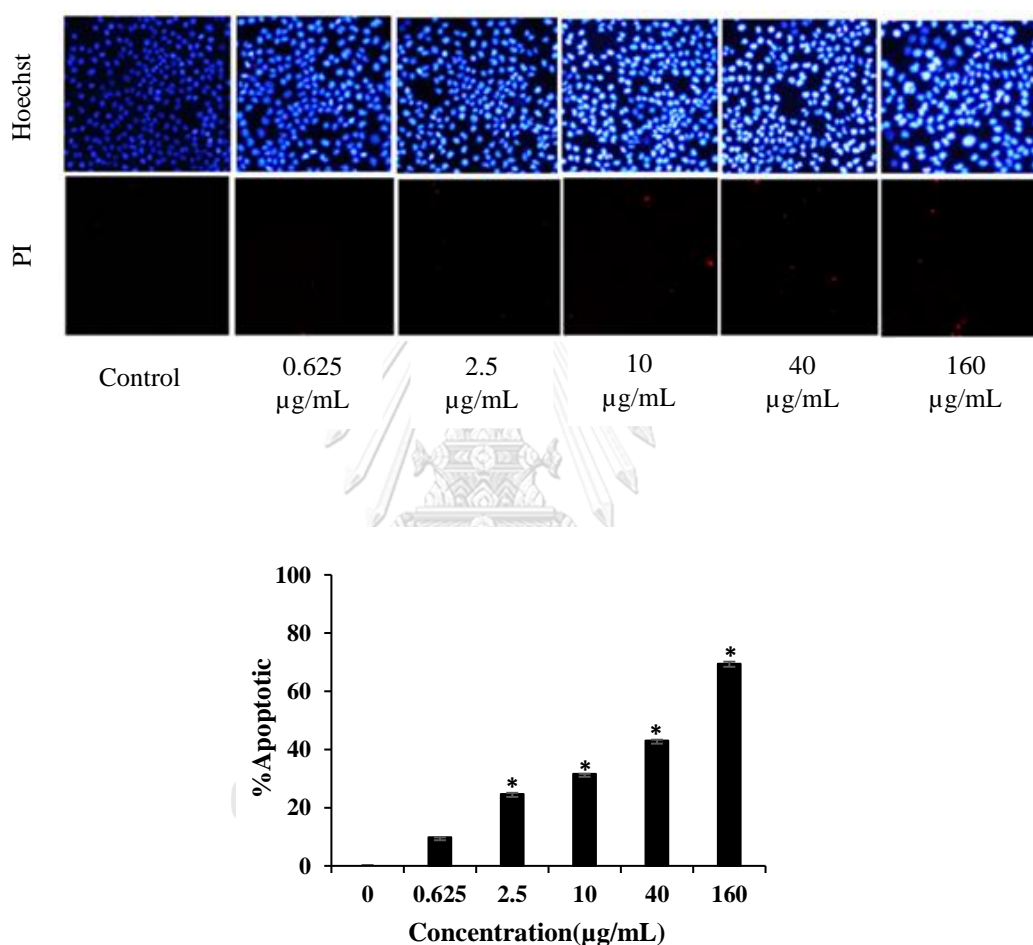


**Figure 9** Evaluation of mode of cell death for ST1-45 in H460 cells using Hoechst and PI staining assay. After treated the cells with ST1-45 for 24 h, the cells were stained. (a) Morphology of the cells was photographed with a fluorescence microscope. (b) The number of apoptotic cells was counted using Image J software. The percentage of apoptotic cell death was significantly increased in a dose-

dependent manner following exposure to the extract. Data obained from averaged values of independent triplicate experiments. *$P$ value ≤ 0.05 versus non-treated control group.

## 2. Selective anticancer activity of ST1-45 in human NSCLC H460 cell line and human keratinocytes cell line (HaCaT)

Although the main purpose of chemotherapy is to kill rapidly proliferating cancer cells, most of the existing chemotherapeutic drugs destroy both cancerous and non-cancerous cells which can result in undesired adverse effects. So, to verify whether ST1-45 possess selective anticancer activity against cancerous cells, human Keratinocyte cells (HaCaT) were used as a non-cancerous cell model. After treated both cell lines with various concentrations of ST1-45 (ranging from 0.3 µg/mL to 5 µg/mL) for 24 h, the cytotoxic effect of the extract was measured by MTT assay. The result indicated that dose-dependent reduction of cell viability was occurred significantly in H460 cells. In contrast, there was no significant changes in cell viability of normal cells. These results collectively revealed that ST1-45 was a potent and selective anticancer compound which contribute to high potential and interesting compound for further investigations (Fig.10).
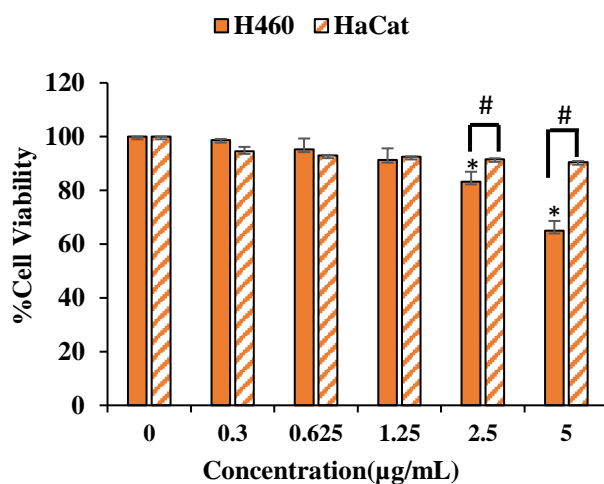
**Figure 10** ST1-45 induce cell death selectively in the H460 cell line compared to non-cancerous HaCaT cells. Data from the average of the five experiments independently ± SD. * $P$ value ≤ 0.05 versus control group. # $P$ value ≤ 0.05 HaCat cells.
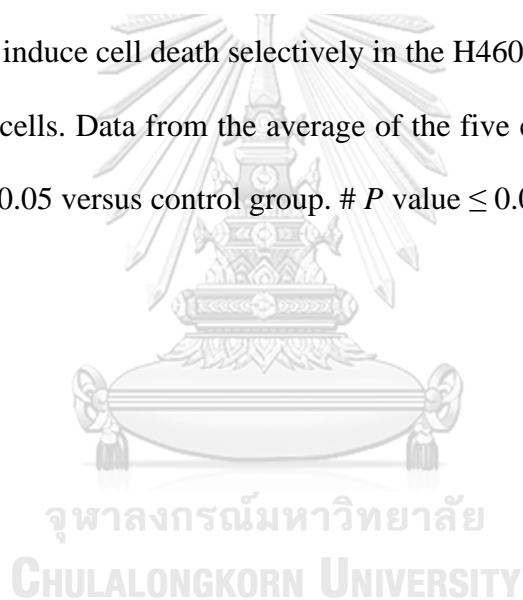
## 3.ST1-45 induced the sensitivity of NSCLC H460 cells to cisplatin

To examine the potential of ST1-45 to augment the chemosensitivity of H460 cells to cisplatin, the cells were pretreated for 1 h with optimal non-toxic dose (1.25 µg/mL) of ST1-45 followed by various dose range of cisplatin for 24 h and measured the cell viability percentage by MTT assay. The results clearly indicated that pretreatment with ST1-45 could sensitize H460 cells to cisplatin treatment with the $IC_{50}$ at 13.65 µM, whereas exhibit $IC_{50}$ at 37.60 µM when treated with cisplatin only (Fig.11).
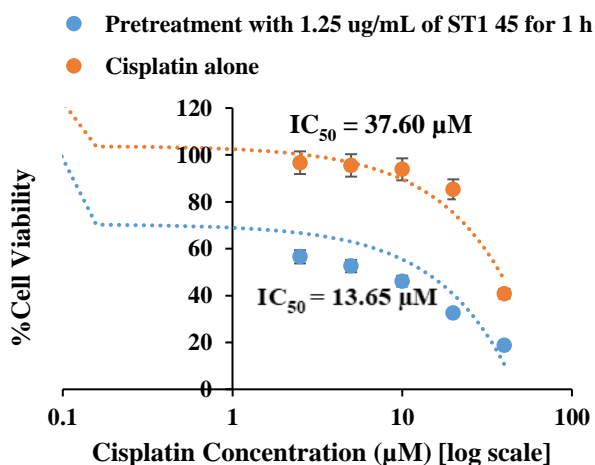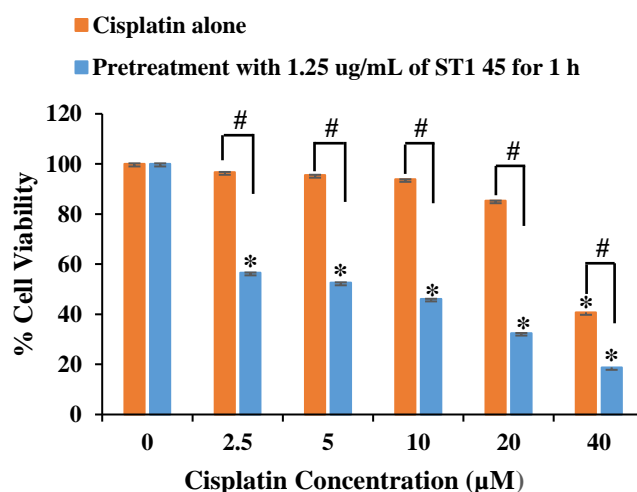
**Figure 11** Sensitizing effect of secondary metabolite from *Streptomyces* on cisplatin-induced apoptosis in human NSCLC H460 cell line. Values are means ± SD of the three independent experiments.*P value ≤ 0.05 versus non-treated control group.#P ≤ 0.05 versus the cells treated with cisplatin alone.

## 4. Synergistic anticancer effect of crude extract ST1-45 and cisplatin

To determine the synergistic interaction between ST1-45 and cisplatin, MTT assay was performed to evaluate cell viability percentage. Then, the results were submitted to synergy finder web-based tool and bliss model was used as reference model to calculate synergy score. If the synergy score is (i) less than -10: the interaction between two drugs is likely to be antagonistic, (ii) from -10 to 10: the interaction between two drugs is likely to be antagonistic, (iii) larger than 10: the interaction between two drugs seems to be synergistic. Based on analyzed results, the bliss synergy score between ST1 45 and cisplatin is 29.946 which shows strong synergistic interaction.
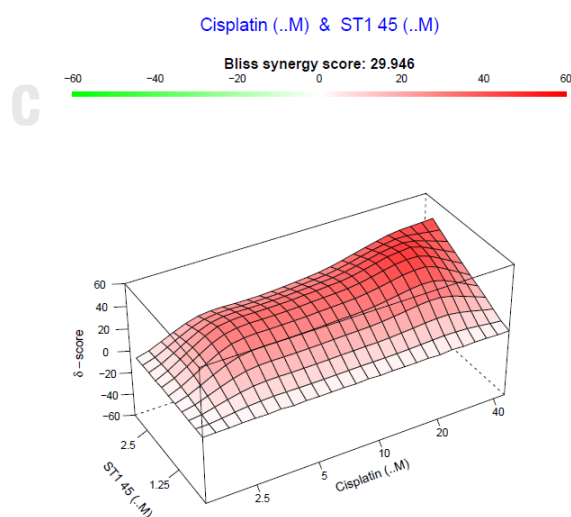


**Figure 122** Bliss synergy score of ST1-45 and cisplatin analyzed by synergy finder

**5.Determination of mode of cell death by flow cytometry analysis**

To ascertain the mode of cell death induced by combined treatment of ST1-45 and cisplatin, the cells were stained with annexin V-FITC/PI and analyzed by flow cytometry. The percentages of cells analyzed by flow cytometry following Annexin V and PI staining could be classified into four categories. The populations of cells residing in the annexin V+/PI- and the annexin V+/PI+ quadrants were determined as early and late apoptotic cells, respectively. The annexin V−/PI - and the Annexin V−/PI+ quadrants were determined as living cells and necrotic cells, respectively. The results in this study showed that the percentage of apoptosis cells were significantly increased in the groups of combined treatment with 1.25 µg/mL of ST1-45 and various concentrations of cisplatin compared to cisplatin alone (Fig.12). Average percentage of the cells in the different mode of cell death after treatment with ST1-45, cisplatin and their combinations are summarized in Table 1.

**Control Cells**

*Unstained H460*
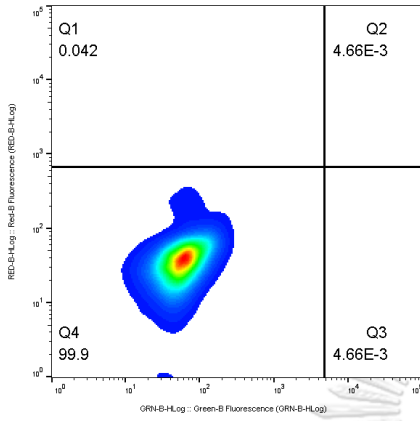


*Annexin only*
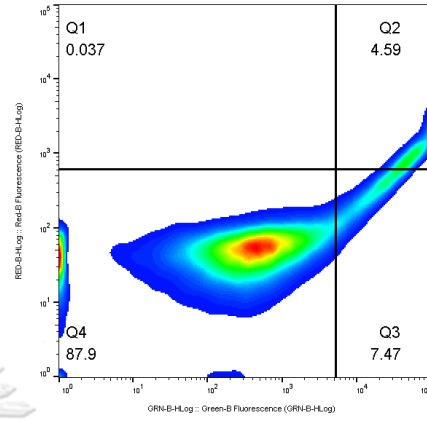


*PI only*
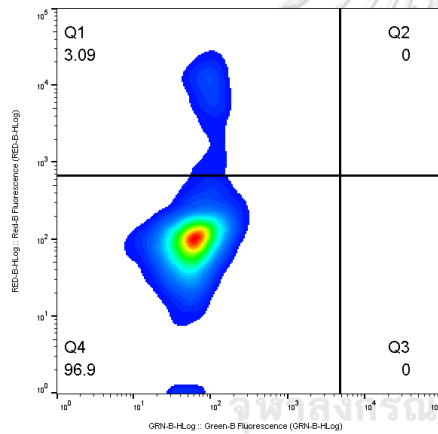


*Annexin V + PI*
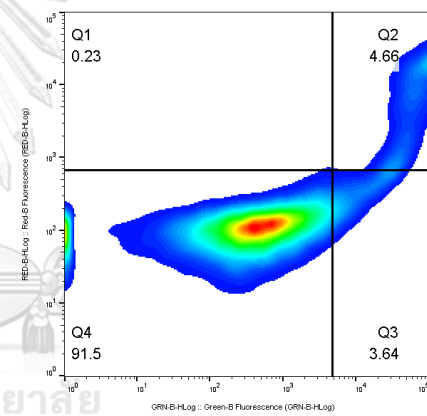


*Annexin V + PI*
*(H₂O₂ 100 µM)*
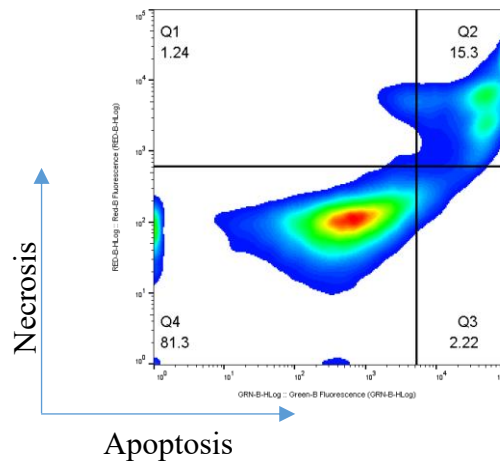
**Treated Cells (Annexin V + PI co-staining)**



*Control*

*1.25 µg/mL (ST1-45)*

*Cisplatin 2.5 µM*

*ST1-45 + Cisplatin 2.5 µM*

*Cisplatin 5 µM*

*ST1-45 + Cisplatin 5 µM*
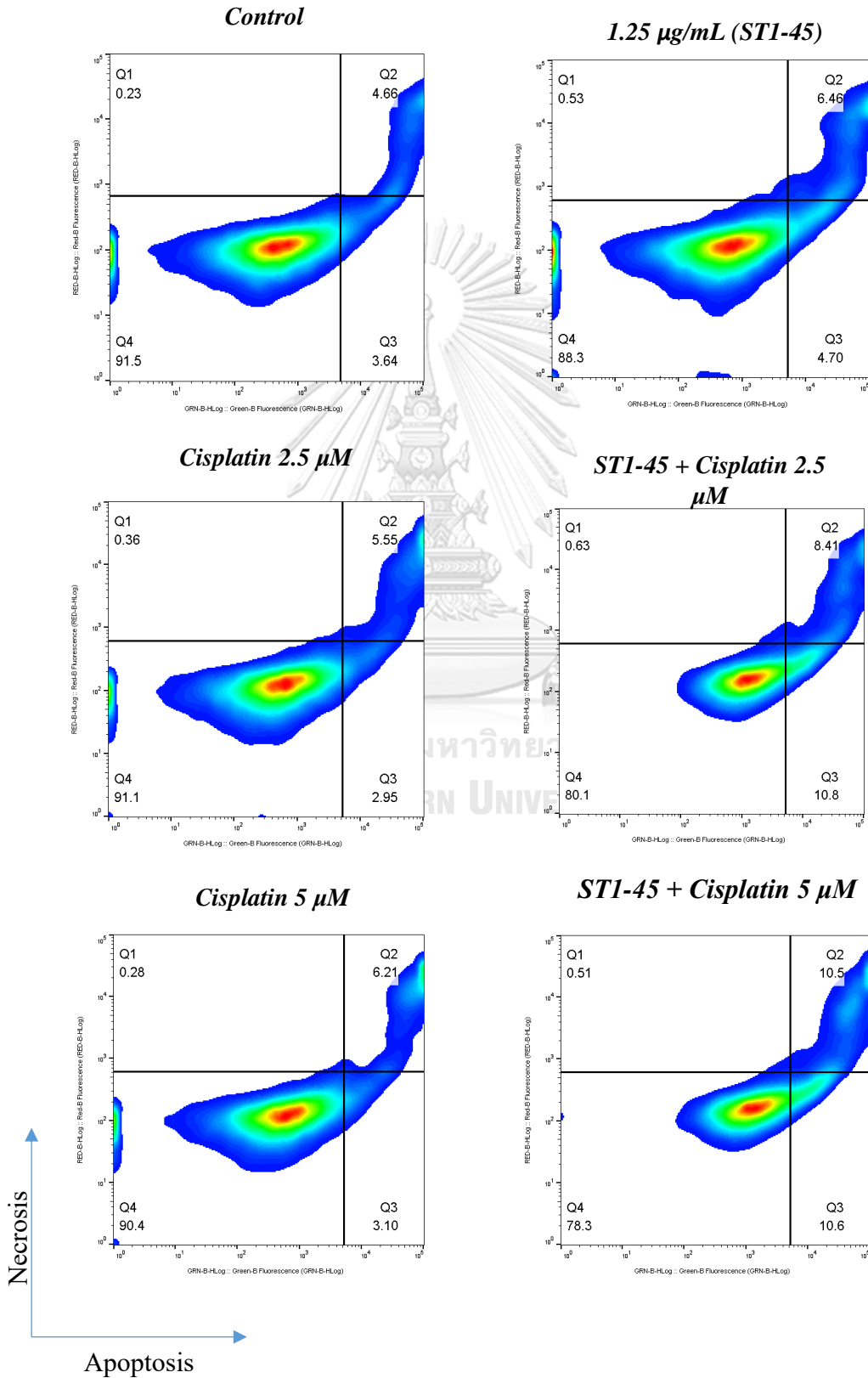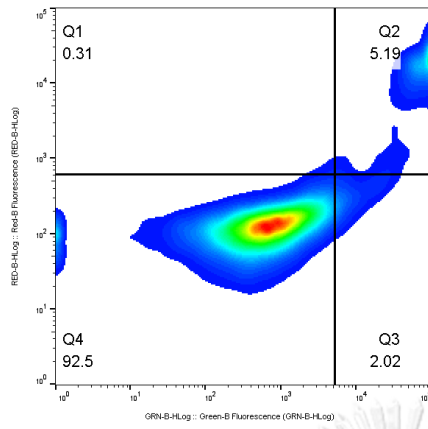
*Cisplatin 10 μM*     *ST1-45 + Cisplatin 10 μM*
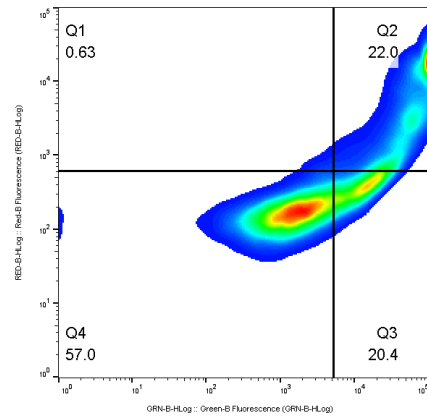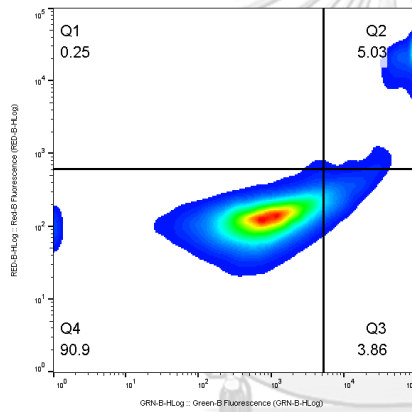


*Cisplatin 20 μM*     *ST1-45 + Cisplatin 20 μM*
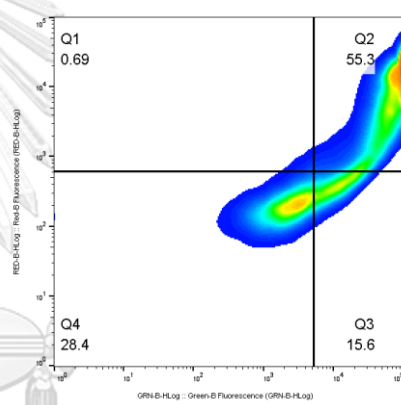


*Cisplatin 40 μM*     *ST1-45 + Cisplatin 40 μM*
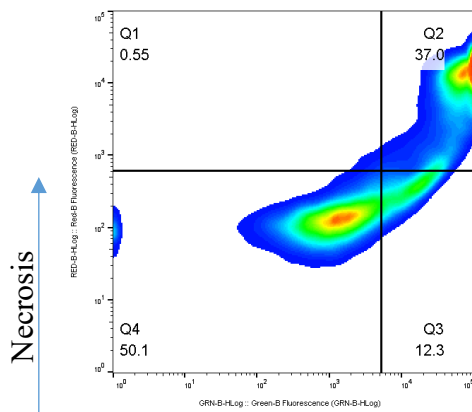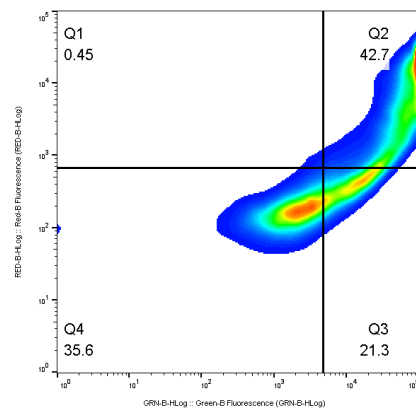
# MODE OF CELL DEATH
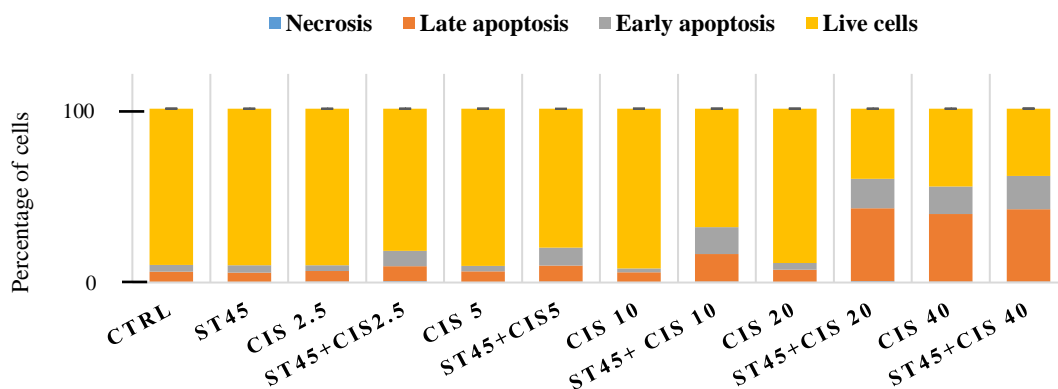


**Figure 13** Apoptosis rate in H460 cells was assessed by flow cytometry using the annexin V-FITC/PI double staining assay after treatment with 1.25 µg/mL of ST1-45, various concentrations of cisplatin and their combinations. The X-axis represents the FITC-labeled annexin V positive cells whereas the Y-axis represents the PI-labeled populations. The Q1 quadrant indicates the percentage of necrotic cells (An - , PI +) , the Q2 quadrant shows the percentage of late apoptotic cells (An +, PI +), the Q3 quadrant indicates the percentage of early apoptotic cells (An +, PI -), and the Q4 quadrant shows normal cells (An -, PI -). The error bars refer to the standard deviations obtained from the triplicate sample analysis.

**Table 1** Average percentage of the cells in the different mode of cell death after treatment with ST1-45, cisplatin and their combinations.

| Samples | Q1 (%) | Q2 (%) | Q3 (%) | Q4 (%) |
|---|---|---|---|---|
| Control | 0.40 ± 0.15 | 5.93 ± 1.75 | 3.78 ± 0.74 | 89.90 ± 2.43 |
| ST1-45 | 0.40 ± 0.09 | 5.33 ± 1.06 | 4.18 ± 0.49 | 90.03 ± 1.62 |
| Cis 2.5 μM | 0.52 ± 0.31 | 6.17 ± 1.56 | 3.21 ± 0.44 | 90.07 ± 1.62 |
| ST1-45 + Cis 2.5 μM | 0.73 ± 0.14 | 8.67 ± 0.37 | 8.88 ± 2.72 | 81.70 ± 2.62*# |
| Cis 5 μM | 0.45 ± 0.22 | 5.99 ± 0.88 | 3.13 ± 0.09 | 90.43 ± 1.15 |
| ST1-45 + Cis 5 μM | 0.49 ± 0.04 | 9.19 ± 1.86*# | 10.35 ± 0.35*# | 79.90 ± 2.26*# |
| Cis 10 μM | 0.34 ± 0.13 | 5.52 ± 2.11 | 2.26 ± 0.87 | 91.87 ± 3.10 |
| ST1-45 + Cis 10 μM | 0.60 ± 0.05 | 15.86 ± 8.68*# | 15.30 ± 7.21*# | 68.25 ± 15.90*# |
| Cis 20 μM | 0.32 ± 0.07 | 7.13 ± 3.03 | 3.73 ± 0.24 | 88.83 ± 3.24*# |
| ST1-45 + Cis 20 μM | 0.74 ± 0.06 | 41.95 ± 18.08*# | 16.90 ± 1.84*# | 40.40 ± 16,97*# |
| Cis 40 μM | 0.48 ± 0.09 | 39.00 ± 2.83*# | 15.70 ± 4.80*# | 44.80 ± 7.50*# |
| ST1-45 + Cis 40 μM | 0.54 ± 0.12 | 41.60 ± 1.56*# | 19.20 ± 2.97*# | 38.70 ± 4.38*# |

*$P$ value ≤ 0.05 versus non-treated control group.

#P ≤ 0.05 versus the cells treated with cisplatin alone.

**6. Molecular mechanism of chemosensitization effect did not correlate with IRE1-mediated ER stress pathway**

We established an experimental approach to whether ER stress mediated apoptosis mechanism might be a possible molecular mechanism of the chemosensitizing effect of ST1-45 on cisplatin-induced apoptosis in H460 cells. Based on our proposed mechanism, IRE1α activated *XBP-1* splicing ratio was firstly determined by RT-PCR analysis. The results demonstrated that the *XBP-1* splicing pattern did not change after treatment with various concentrations of ST1-45 (Fig.13). In our subsequent western blot analysis, the phosphorylated IRE1 α expression level remains unchanged in both groups of ST1-45 alone and combination with non-significant dose of cisplatin ranging from 2.5 μM to 10 μM (Fig.14). Interestingly, although pIRE1 α protein level did not alter, upregulation of pJNK expression level was prominently found in a single treatment with ST1-45 and cotreatment of ST1-45 with cisplatin at 10 μM whereas there was no difference in the total protein level of JNK. Altogether, the underlying apoptotic mechanism of sensitizing effect perhaps due to other upstream signaling pathways that lead to JNK activation, independent of the IRE1 α-mediated ER stress pathway.
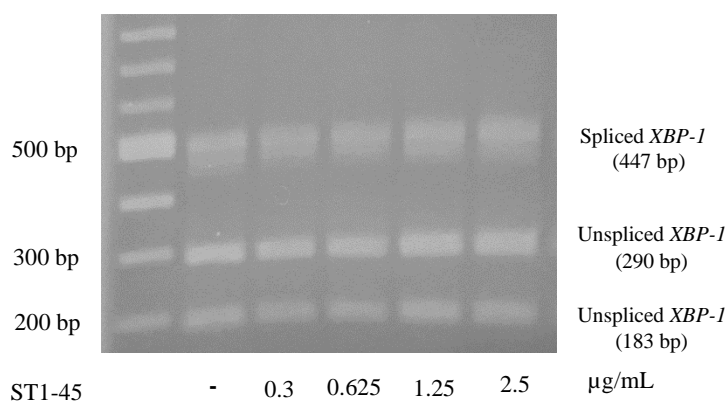
**Figure 14** RT PCR analysis for secondary metabolites of *Streptomyces* sp. ST1-45.The cDNA from total RNA from these cells was subjected to PCR and *Pst1* restriction digestion (CTGCA|G) to semi-quantitatively evaluate the levels of *XBP-1s*. Data were expressed as means ± s.d. (n=3).

**(a)**

**(b)**
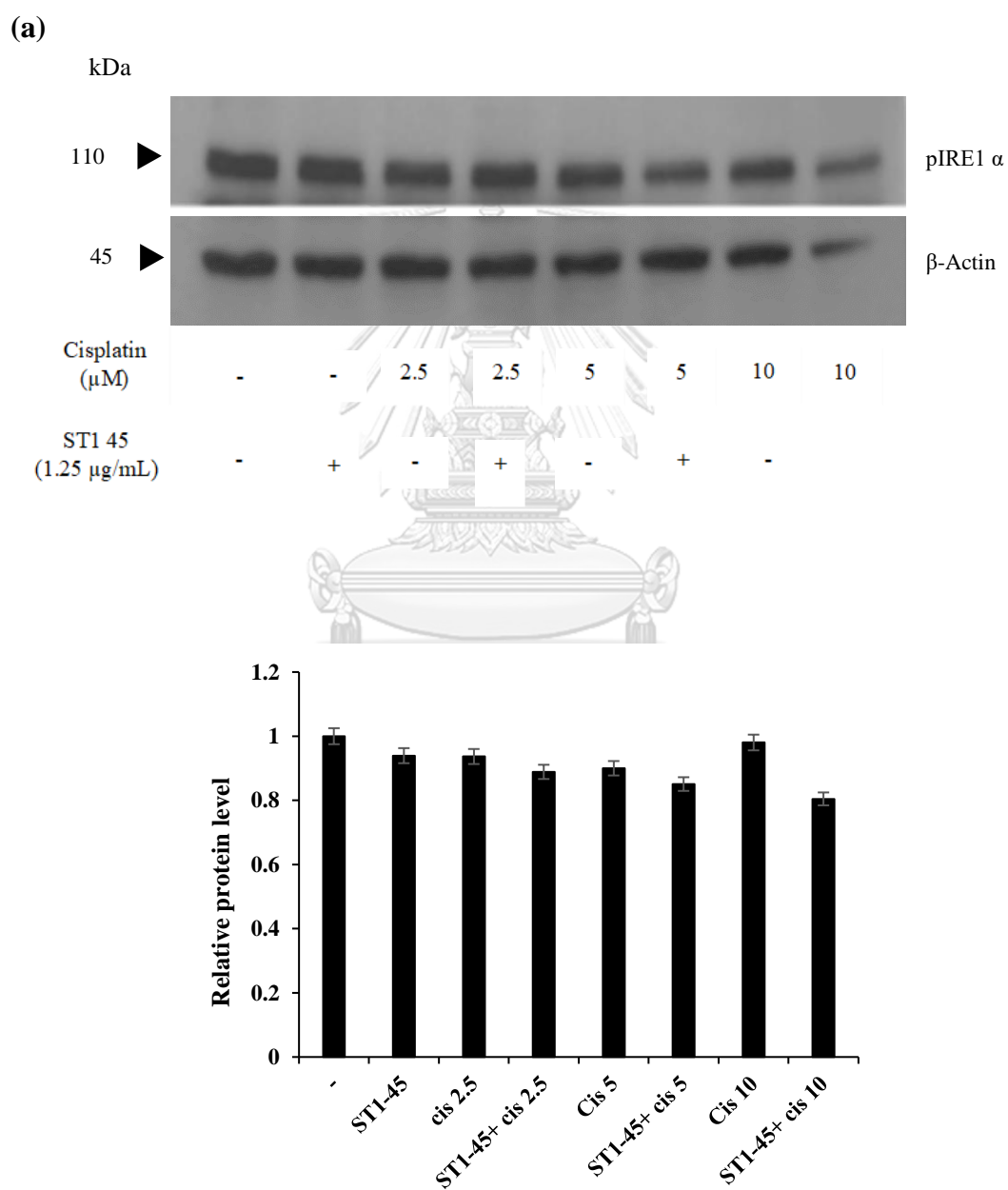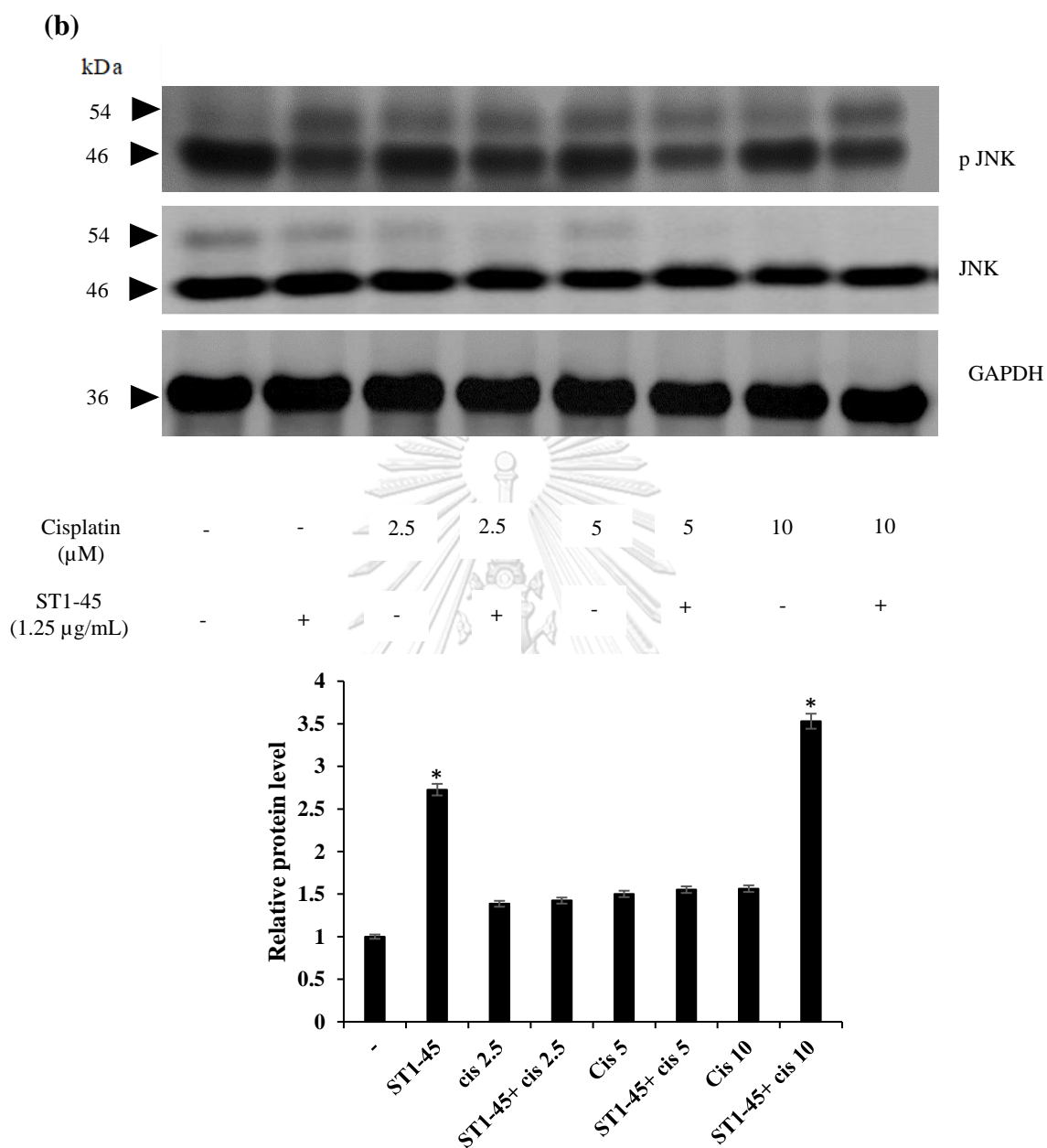


Figure 15 Evaluation of ER stress protein level by western blot analysis after

pretreatment with 1.25 µg/mL of ST1-45 on cisplatin treated H460 lung cancer cells

(a) expression level of ER stress marker, pIRE1 α  (b) phosphorylated and total JNK

proteins expression level. Values are means ± SD of the three independent experiments. *$P$ value ≤ 0.05 versus non-treated control group.

**7.Strain identification by 16S rRNA gene analysis**

BLAST analysis based on almost complete 16S rRNA gene of ST1-64 and ST1-54 exhibited the strain closely correlated with *Streptomyces lucensis* NBRC 13056[T] (99.20%), and *Streptomyces glomeratus* LMG19903[T] (99.69%) respectively. However, the 16S rRNA result of ST1-45 did not provide sufficient information to identify the strain accurately. So, the whole genome sequence analysis of ST1-45 was conducted for strain identification concisely.

**8.Whole Genome Sequencing for ST1-45**

The genome sequence of ST1-45 was submitted to TYGS server to identify strain and construct the phylogenomic tree. Based on the phylogenomic tree analysis, strain ST1-45 shared the same node with *Streptomyces puniciscabiei* DSM 41929[T] and shared the cluster with the other five *Streptomyces* comprising *Streptomyces fodineus* TW1S1[T], *Streptomyces durhamensis* NRRL B-3309[T], *Streptomyces alanosinicus* JCM 4714[T], and *Streptomyces yokosukanensis* DSM 40224[T] (Fig.15).

The comparative genome analysis results demonstrated that strain ST1-45 exhibited ANI and DNA-DNA hybridization values in the range of 85.83% - 92.33% and 37.4% - 47.5%, respectively. These values were lower than the recommended cut-off value, 95-96% of ANI, and 70% of dDDH for delineating species (Table 2) (147, 148). Hence, it can be postulated that strain ST1-45 represents the candidate for novel *Streptomyces* species based on above genomic evidence. However, to propose the

description of new species, it is strongly recommended to perform polybasic taxonomic studies to confirm new specie.
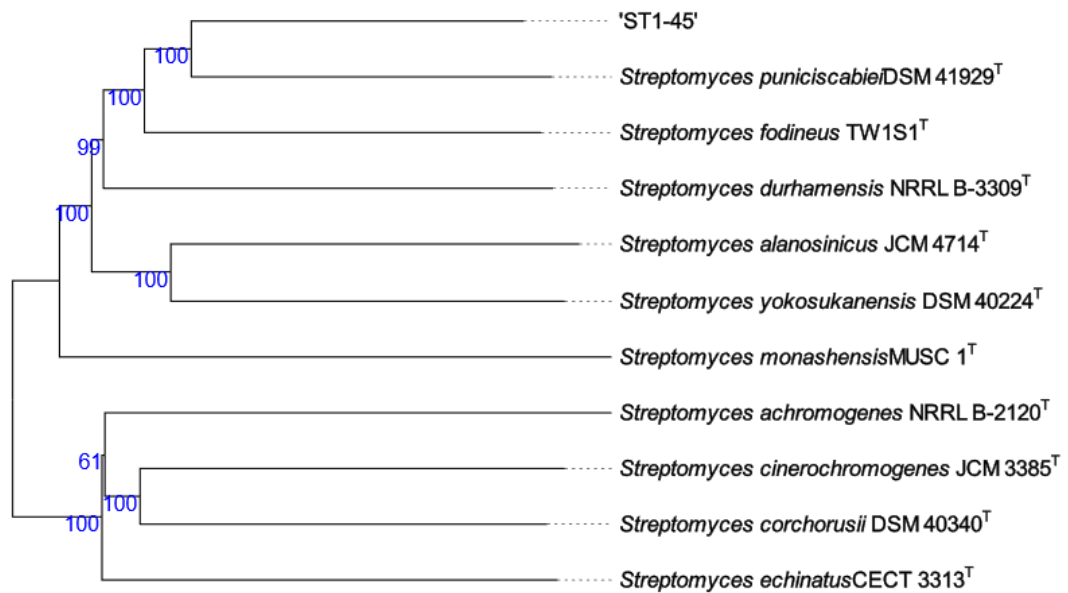


**Figure 16** The phylogenetic tree based on genome sequence of strain ST1-45 and related *Streptomyces* type strain available on the TYGS database. The number at the node are GBDP pseudo-bootstrap support values obtained from 100 replication.

**Table 2** ANIb, ANIm values (%) and the digital DNA-DNA hybridization (dDDH)

values between the draft genomes of strain ST1-45 and related *Streptomyces* species.

| Strain | Genome size (bp) | % G+C content | Compare to ST1-45 | | |
|---|---|---|---|---|---|
| | | | % dDDH | ANIb% | ANIm% |
| ST1-45 | 8,937,732 | 71.10 | - | - | - |
| *S. fodineus* TW1S1[T] | 9,698,948 | 71.09 | 42.3 | 88.94 | 91.42 |
| *S. durhamensis* NRRL B-3309[T] | 9,311,708 | 71.69 | 40.7 | 87.81 | 90.56 |
| *S. alanosinicus* JCM 4714[T] | 10,244,856 | 70.90 | 35.7 | 86.95 | 90.01 |
| *S. monashensis* MUSC 1[T] | 10,254,857 | 71.50 | 35.9 | 85.83 | 89.11 |
| *S. puniciscabiei* DSM 41929[T] | 9,146,138 | 71.40 | 47.5 | 90.15 | 92.33 |
| *S. yokosukanensis* DSM 40224[T] | 10,159,272 | 70.90 | 37.4 | 87.37 | 90.18 |

## 9.Distribution of secondary metabolite biosynthetic gene cluster in *Streptomyces* sp. ST1-45

AntiSMASH server is a useful software pipeline for the determination of biosynthetic secondary metabolite gene clusters in the genome of strain ST1-45. Based on antiSMASH pipeline, strain ST1-45 possesses several secondary metabolite biosynthetic gene clusters including melanin, siderophore, geosmin, bacteriocin, ectoine, terpene, NRPS, T1PKS, T2PKS, and T3PKS. Three clusters showed 100% similarity with the known biosynthetic gene cluster, including geosmin, ectoine, and albaflavenone (Table 3). Interestingly, some of the gene clusters showed low similarity percentage with secondary metabolites which have been identified. Thus,

strain ST1-45 might produce unknown secondary metabolites that have not been proposed.

Geosmin is a sesquiterpene compound that has an earthy or musty odor produced by various types of microorganisms such as cyanobacteria and filamentous bacteria, especially the *Streptomyces*. The earthy and musty smell of the geosmin is responsible for commercially freshwater fish such as catfish and Nile-tilapia as well as the drinking water.

Ectoine which is a naturally produced cyclic tetrahydropyrimidine organic osmolyte is a compatible solute, and protective substance. This compound is produced by many species of bacteria and involved in the surviving role of organisms under osmotic stress. Ectoine is used as an active constituent in sun protection and skincare products.

Albaflavenone which was firstly isolated from *Streptomyces albidoflavus* is a β unsaturated sesquiterpene ketone. The compound has a smell of earthy and camphor-like odor. Albaflavenone has antibacterial activity against Bacillus subtilis with a MIC value of 10 µg/ml (149).

**Table 3** The distribution of the biosynthetic gene cluster in *Streptomyces* sp. ST1-45.

| Cluster | Type | Most similar known cluster (class) | Similarity (%) |
|---|---|---|---|
| 1 | melanin | Melanin | 60 |
| 2 | Siderophore | desferrioxamin B/desferrioxamine E | 83 |
| 3 | Siderophore | Grincamycin (polyketide: type II + saccharide:hybrid/tailoring) | 5 |
| 4 | Geosmin | Terpene | 100 |
| 5 | Bacteriocin | Informatipeptin (RiPP: Lanthipeptide) | 42 |
| 6 | NRPS | Arginomycin | 10 |
| 7 | HgIE-KS, T1PKS | Cinnamycin (RiPP:Lanthipeptide) | 19 |
| 8 | T3PKS | Herboxidiene | 8 |
| 9 | T3PKS | Daptomycin (NRP) | 9 |
| 10 | T2PKS | Hiroshidine (Polyketide) | 27 |
| 11 | terpene | Hopene (terpene) | 92 |
| 12 | T1PKS | Heronamides A-F (NRP + polyketide) | 54 |
| 13 | NRPS | Pepticinnamin E (NRP + polyketide) | 10 |
| 14 | NRPS, T1PKS | Foxicins A-D (NRP + polyketide) | 9 |
| 15 | Ectoine | Ectoine | 100 |
| 16 | Siderophore | Ficellomycin (NRP) | 3 |
| 17 | NRPS, bacteriocin | Vazabitide A (NRP) | 15 |
| 18 | Terpene | Albaflavenone (terpene) | 100 |
| 19 | T1PKS | Hitachimycin (polyketide) | 31 |
| 20 | T1PKS | Lydicamycin (NRP + polyketide: modular type 1) | 32 |

**ST1-45**

**albaflavenone biosynthetic gene cluster from *Streptomyces coelicolor* A3 (BGC0000660)**

**ST1-45**

**ectoine biosynthetic gene cluster from *Streptomyces anulatus* (BGC0000853)**

CHULALONGKORN UNIVERSITY

**ST1-45**

**geosmin biosynthetic gene cluster from *Streptomyces coelicolor* A3 (BGC0001181)**
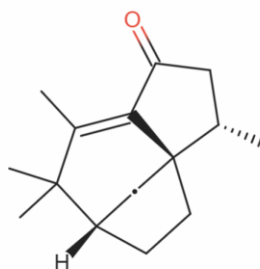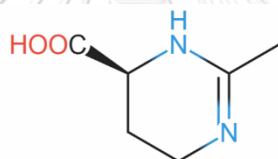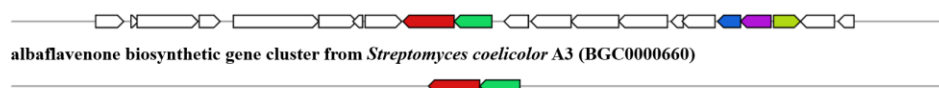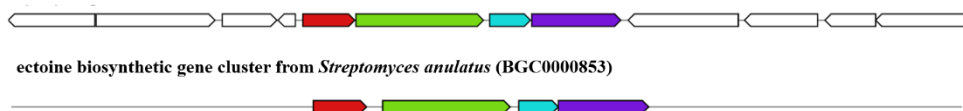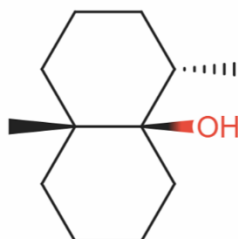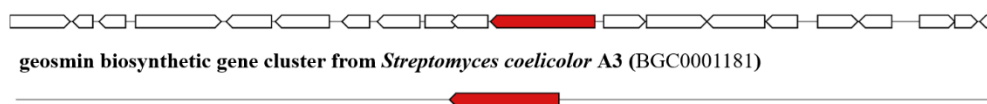
**10.TLC Analysis**

TLC profile for ethyl acetate extract of ST1-45 was shown in (Fig.16). The results obtained showed the purple spot after derivatization with p-anisaldehyde reagent which indicate the presence of phenol, terpenes, and sugars. Blue spots were appeared on the TLC plate derivatized with phosphomolybdic acid which represent the presence of steroids. Tan-brown color spot was appeared on the TLC plate after exposure with iodine vapor representing the presence of hydrocarbons. Moreover, after the plate was derivatized with 10% sulfuric acid in methanol and 50% Sulfuric acid in water and then visualized under long wave UV (366 nm), fluorescence spots were detected. This testing also indicates the presence of hydrocarbons. However, the crude extract did not contain alkaloids and amines since red spot did not show in the TLC plate after spray with Dragendorff reagent and ninhydrin respectively.

**Table 4** TLC results of ST1-45

| No. | Detection Method | No: of spot | $R_f$ value |
|-----|------------------|-------------|-------------|
| 1.  | p-anisaldehyde sulfuric acid | 2 | 0.43, 0.57 |
| 2.  | Phosphomolybdic acid | 2 | 0.38, 0.49 |
| 3.  | Iodine vapor | 1 | 0.29, 0.43, 0.53 |
| 4   | Sulfuric acid/ methanol/ LWUV | 3 | 0.25, 0.35, 0.47 |
| 5.  | Sulfuric acid/ LWUV | 1 | 0.41 |
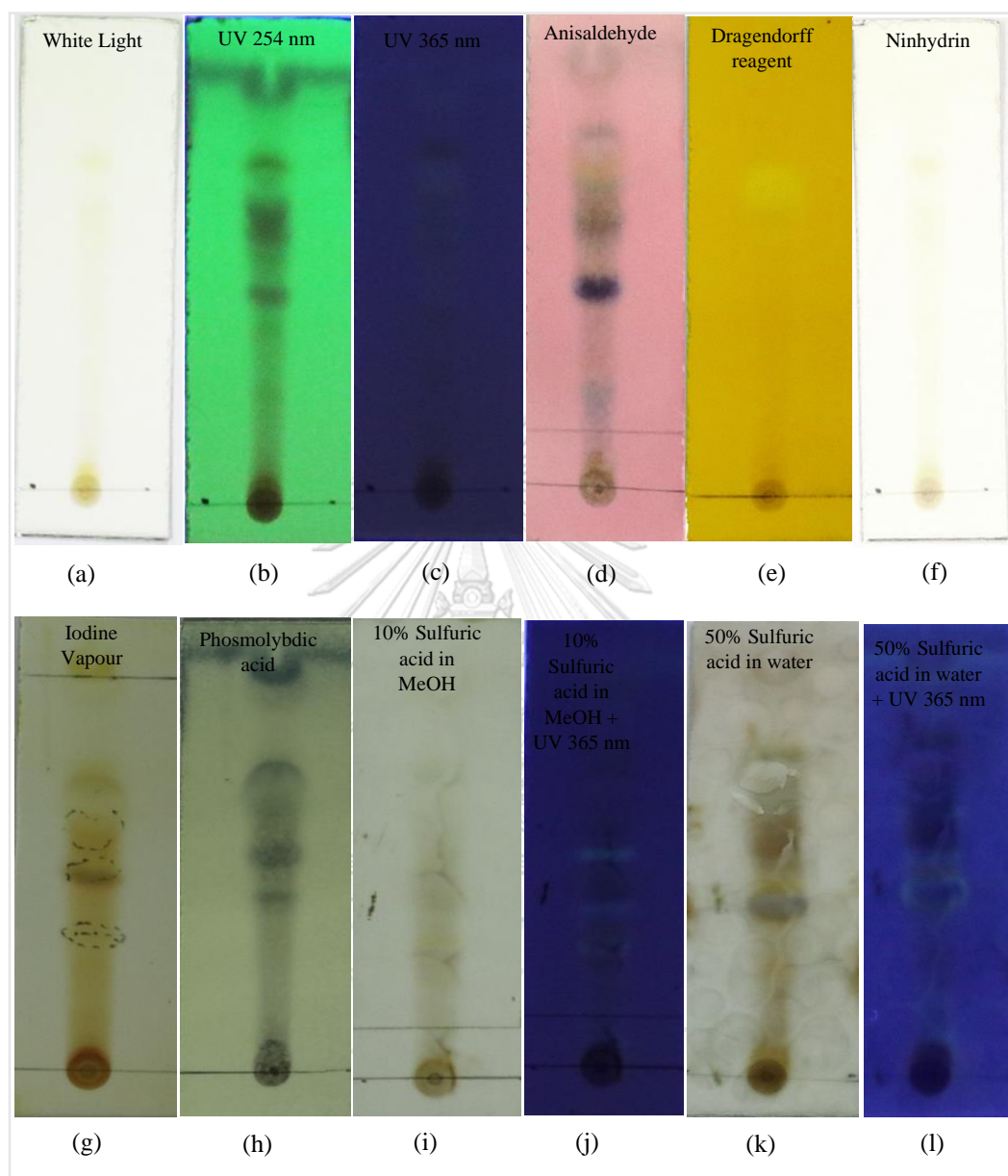
**Figure 17** TLC profile of ST1-45 isolated from novel *Streptomyces* sp.(a) viewed with normal white light (b) UV 254 nm (c) UV 365 nm (d) derivatization with anisaldehyde (e) Dragendorff reagent (f) Ninhydrin (g) Iodine vapour (h) Phosmolybdic acid (i) 10% sulfuric acid in methanol (j) 10% sulfuric acid in methanol with UV 365 nm (k) 50% Sulfuric acid in water (l) 50% sulfuric acid in water with UV 365 nm.

# CHAPTER V

# DISCUSSION AND CONCLUSION

Lung cancer is the foremost wide-reaching cancer-related mortality in the world (2). Although several kinds of antitumor compounds have been developed, their awful adverse effects and drug resistance restrict their benefits in cancer treatment (149,150). Thus, researchers expressed interest in seeking new biologically active metabolites or chemosensitizing agents that can increase the efficacy of standard chemotherapy from natural sources offering fewer toxic effects than current chemotherapeutic drugs. *Streptomyces* have attracted great attention since they shelter different gene clusters that produce different compounds with diverse chemical backbones (151). Through this study, we found the selective and chemosensitizing activites of *Streptomyces* crude extract ST1-45 on cisplatin-induced apoptosis in H460 NSCLC cells.

In our current study, total of eight strains were isolated from the soil of peat swamp forest, Yala Province, Thailand which provide unique and chemically diverse bioactive compounds. Only three of them which showed good purity results based on 16S rRNA sequencing analysis were selected for testing of cytotoxic activities. Our preliminary results demonstrated that ST1-45 possessed potent anticancer activity with $IC_{50}$ value of 9.51 µg/mL whereas the remaining two extracts (ST1-64 and ST1-54) showed cytotoxic effects only at higher concentrations with $IC_{50}$ values of 337.37 µg/mL and 171.52 µg/mL respectively. Thus, we assumed that ST1-45 has potent anticancer activity against H460 lung cancer cells (Fig.8). Next, we were wondering if this extract has the selective cytotoxic effect on cancerous cells without toxic effect

to non-cancerous cells. To verify this possibility, we performed cell viability assay on both cell lines and human keratinocyte cells (HaCat) was used as a non-cancerous cell model in this study. Interestingly, the result exhibited that the percentage of cell viability was significantly reduced on tumorigenic H460 cell line in a dose dependent manner whereas there was not occurred toxic effect in non-tumorigenic HaCaT cell line within the same dose range. According to this result, our findings provide evidence that ST1-45 crude extract isolated from *Streptomyces* sp. could be a potential antitumor compound which exert selective anticancer effect without harmful effect on normal cells (Fig.10).

In our subsequent analysis, the optimal non-toxic dose (1.25 µg/mL) of crude extract ST1-45 was selected for the pre-treatment of H460 cells for 1 h followed by the treatment of various concentrations of cisplatin to evaluate the sensitizing effect of ST1-45 on cisplatin treatment in lung cancer by MTT assay. The results showed that combination of ST1-45 and cisplatin ($IC_{50}$ = 13.65 µM) was more sensitized to NSCLC cells than cisplatin alone ($IC_{50}$ = 37.60 µM) (Fig.11). Additionally, the cells were costained with annexin V and PI whether to investigate the possible induction of cell death (apoptosis and/or necrosis). The annexin V/PI staining assay allows the simultaneous determination of early apoptosis events depended on annexin V binding to exposed PS and late apoptotic/dead events through the uptake of propidium iodide annexin V, a Ca 2+ dependent phospholipid-binding protein possesses a high affinity for phosphatidyl serine (PS) which is a membrane-bound component localizing in the inner surface of the cell membrane. Translocation of PS from the inner leaflet to the outer surface of the membrane is an indicator of early-stage apoptosis (152). Our

analysis of annexin V and PI staining by flow cytometry analysis illustrated that the increased percentage of early and late phase apoptotic cells was found in the group of combined treatment with ST1-45 and cisplatin in comparison with the group with cisplatin alone. The investigations in this study strongly confirmed that the sensitizing effect of ST1-45 on cisplatin treated cells was due to the activation of apoptosis (Fig. 12).

From the results of RT-PCR and western blot analysis (Fig.13,14), the underlying molecular mechanism of sensitizing effect did not depend on IRE1 α-mediated ER stress mechanism. In our proposed mechanism, non-toxic concentration at 1.25 μg/ml could induces IRE1 α mediated *XBP-1* splicing which is the marker for mild ER stress condition but it is insufficient for apoptotic induction at this dose. When combine with cisplatin, however, the ER stress level will drastically increase, and this high ER stress can trigger JNK activation which will result in apoptotic induction. So, we performed RT-PCR analysis to determine the splicing ratio of *XBP-1*. Unfortunately, we found that there were no changes of *XBP-1* splicing pattern in cells treated with various concentrations of ST1-45 compared to control. Moreover, the expression level of one of the ER stress marker protein (pIRE1 α) which is an upstream regulator of *XBP-1* splicing and JNK activation did not alter in combined treatment with ST1-45 and cisplatin compared to ST1-45 or cisplatin treated alone. Interestingly, we have discovered that overexpression of pJNK protein was found in cells treated with ST1-45 and cotreated with cisplatin at 10 μM compared to control. Although significant cytotoxic effect of ST1-45 was not observed at 1.25 μg/mL, pJNK protein expression was upregulated in immunoblot analysis. Ventura JJ, et al.

reported that transient activation of JNK promotes cell survival, while prolonged JNK activation trigger cellular apoptosis (153). From the results in our study, JNK activation induced by ST1-45 alone might be transient and when combined with genotoxic effect of cisplatin, these combined activities could make the cells prolonged JNK activation which lead to apoptosis (Fig.14). Taken together, the apoptotic mechanism of chemosensitizing effect might come from other upstream signaling pathways for instance MAPK signaling pathway which lead to JNK activation. Based on literature reviews, *Streptomyces* sp. metabolite can induce Bax mediated intrinsic apoptosis and autophagy by inhibition of mTOR pathway in cervical cancer cell lines (154). Neoantimycin F (NAT-F) isolated from *Streptomyces conglobatus* induced apoptosis of non–small cell lung cancer (NSCLC) cells by up-regulating pro-apoptotic protein Bax and downregulating anti-apoptotic protein Bcl-2, Mcl-1, and Bcl-x$_L$, which contribute to cytochrome c release from mitochondria and sequential activation of caspase-9 and -3, as well as the cleavage of poly (ADP-ribose) polymerase. Meanwhile, extracellular signal-regulated kinase (ERK), p38 MAPK (p38), and JNK signaling pathway were also involved in anti-cancer activity of NAT-F in NSCLC cells (155). Therefore, the above-mentioned signaling pathways might be involved in the antitumor activity of ST1 45 in human H460 lung cancer cells and could be promising target for further investigations. Obviously, additional studies will be required to confirm the underlying mechanism of sensitizing effect.

In this study, strain identification of ST1-45 by whole genome sequence analysis revealed that the strain ST1-45 might represent the potential candidate of new species. However, polyphasic taxonomic studies should perform to propose the

description of new species. The potential biosynthetic secondary metabolites gene clusters were evaluated by using antiSMASH software. The presence of geosmin, ectoine, terpene, PKS 1 and NRPS genes in strain ST1-45 suggests the possibility that it can produce bioactive secondary metabolites belonging to these classes of natural products. Therefore, it is important to investigate the major constituents presented in ST1-45 which might potentially be developed as a cytotoxic drug.

In conclusion, the observations from this study provided candidate for novel *Streptomyces* species isolated from peat swamp forest in Yala Province, Thailand possessing anticancer and chemosensitizing activities in H460 human non-small cell lung cancer. This study also sought to address the potential mechanistic aspect underlying the observed sensitizing response of *Streptomyces* crude extract on cisplatin-induced apoptosis via modulation of JNK activation. This opens new avenues to isolation and structural elucidation of active constituents and subsequent evaluation of therapeutic effects of pure isolates in management of cancer. Additionally, this study warrants further experiments to evaluate the exact molecular mechanism for sensitizing effect of ST1-45 on cisplatin-induced apoptosis in H460 lung cancer cells.

# REFERENCES

1.      Hsu PP, Sabatini DM. Cancer cell metabolism: Warburg and beyond. Cell. 2008;134(5):703-7.

2.      McGuire S. World Cancer Report 2014. Geneva, Switzerland: World Health Organization, International Agency for Research on Cancer, WHO Press, 2015. Adv Nutr. 2016;7(2):418-9.

3.      Keith RL, Miller YE. Lung cancer chemoprevention: current status and future prospects. Nat Rev Clin Oncol. 2013;10(6):334-43.

4.      Hirsch FR, Lippman SM. Advances in the biology of lung cancer chemoprevention. J Clin Oncol. 2005;23(14):3186-97.

5.      Dela Cruz CS, Tanoue LT, Matthay RA. Lung cancer: epidemiology, etiology, and prevention. Clin Chest Med. 2011;32(4):605-44.

6.      Salgia R, Skarin AT. Molecular abnormalities in lung cancer. J Clin Oncol. 1998;16(3):1207-17.

7.      Maconachie R, Mercer T, Navani N,et al. Lung cancer: diagnosis and management: summary of updated NICE guidance. BMJ. 2019;364:l1049.

8.      Kotecha R, Takami A, Espinoza JL. Dietary phytochemicals and cancer chemoprevention: a review of the clinical evidence. Oncotarget. 2016;7(32):52517-29.

9.      Marciniak SJ. Endoplasmic reticulum stress in lung disease. Eur Respir Rev. 2017;26(144): 617-18.

10.     Mann MJ, Hendershot LM. UPR activation alters chemosensitivity of tumor cells. Cancer Biol Ther. 2006;5(7):736-40.

11.     Ma Y, Hendershot LM. The role of the unfolded protein response in tumour development: friend or foe? Nat Rev Cancer. 2004;4(12):966-77.

12.    Wang S, Kaufman RJ. How does protein misfolding in the endoplasmic reticulum affect lipid metabolism in the liver? Curr Opin Lipidol. 2014;25(2):125-32.

13.    Avril T, Vauleon E, Chevet E. Endoplasmic reticulum stress signaling and chemotherapy resistance in solid cancers. Oncogenesis. 2017;6(8):e373.

14.    Maurel M, McGrath EP, Mnich K, et al. Controlling the unfolded protein response-mediated life and death decisions in cancer. Semin Cancer Biol. 2015;33:57-66.

15.    Wang M, Law ME, Castellano RK, et al. The unfolded protein response as a target for anticancer therapeutics. Crit Rev Oncol Hematol. 2018;127:66-79.

16.    Ai X, Guo X, Wang J, et al. Targeted therapies for advanced non-small cell lung cancer. Oncotarget. 2018;9(101):37589-607.

17.    Loehrer PJ, Einhorn LH. Drugs five years later. Cisplatin. Ann Intern Med. 1984;100(5):704-13.

18.    Reedijk J. New clues for platinum antitumor chemistry: kinetically controlled metal binding to DNA. Proc Natl Acad Sci U S A. 2003;100(7):3611-6.

19.    Mandic A, Hansson J, Linder S, et al. Cisplatin induces endoplasmic reticulum stress and nucleus-independent apoptotic signaling. J Biol Chem. 2003;278(11):9100-6.

20.    Yu F, Megyesi J, Price PM. Cytoplasmic initiation of cisplatin cytotoxicity. Am J Physiol Renal Physiol. 2008;295(1):F44-52.

21.    Martins I, Kepp O, Schlemmer F, et al. Restoration of the immunogenicity of cisplatin-induced cancer cell death by endoplasmic reticulum stress. Oncogene. 2011;30(10):1147-58.

22.     Xu Y, Wang C, Li Z. A new strategy of promoting cisplatin chemotherapeutic efficiency by targeting endoplasmic reticulum stress. Mol Clin Oncol. 2014;2(1):3-7.

23.     Ventura M, Canchaya C, Tauch A, et al. Genomics of Actinobacteria: tracing the evolutionary history of an ancient phylum. Microbiol Mol Biol Rev. 2007;71(3):495-548.

24.     Bérdy J. Bioactive Microbial Metabolites. J. Antibiot. 2005;58(1):1-26.

25.     Tan LT-H, Chan K-G, Lee L-H,et al. *Streptomyces* Bacteria as Potential Probiotics in Aquaculture. Front. Microbiol. 2016;7(79).

26.     Grimm A, Madduri K, Ali A, et al. Characterization of the *Streptomyces peucetius* ATCC 29050 genes encoding doxorubicin polyketide synthase. Gene. 1994;151(1-2):1-10.

27.     Du L, Sanchez C, Chen M,et al. The biosynthetic gene cluster for the antitumor drug bleomycin from *Streptomyces verticillus* ATCC15003 supporting functional interactions between nonribosomal peptide synthetases and a polyketide synthase. Chem Biol. 2000;7(8):623-42.

28.     Limonta P, Moretti RM, Marzagalli M,et al. Role of endoplasmic reticulum stress in the anticancer activity of natural compounds. Int J Mol Sci. 2019;20(4): 961.

29.     Kim C, Song HS, Park H, et al. Activation of ER stress-dependent miR-216b has a critical role in *Salvia miltiorrhiza* ethanol-extract-induced apoptosis in U266 and U937 cells. Int J Mol Sci. 2018;19(4): 1240.

30.     Cha JA, Song HS, Kang B, et al. miR-211 plays a critical role in *Cnidium officinale* makino extract-induced, ROS/ER stress-mediated apoptosis in U937 and U266 Cells. Int J Mol Sci. 2018;19(3): 865.

31.    Park SK, Sanders BG, Kline K. Tocotrienols induce apoptosis in breast cancer cell lines via an endoplasmic reticulum stress-dependent increase in extrinsic death receptor signaling. Breast Cancer Res Treat. 2010;124(2):361-75.

32.    Wang Y, Ha M, Liu J, et al. Role of BCL2-associated athanogene in resistance to platinum-based chemotherapy in non-small-cell lung cancer. Oncol. lett. 2015;11: 984-990.

33.    Ahmad M, Hahn IF, Chatterjee S. GRP78 up-regulation leads to hypersensitization to cisplatin in A549 lung cancer cells. Anticancer Res. 2014;34(7):3493-500.

34.    Scott WJ, Howington J, Feigenberg S, et al. Treatment of non-small cell lung cancer stage I and stage II: ACCP evidence-based clinical practice guidelines (2nd edition). Chest. 2007;132(3 Suppl):234S-42S.

35.    Ramalingam S, Belani C. Systemic chemotherapy for advanced non-small cell lung cancer: recent advances and future directions. Oncologist. 2008;13 Suppl 1:5-13.

36.    Go RS, Adjei AA. Review of the comparative pharmacology and clinical activity of cisplatin and carboplatin. J Clin Oncol. 1999;17(1):409-22.

37.    Wang D, Lippard SJ. Cellular processing of platinum anticancer drugs. Nat. Rev. Drug. Discov. 2005;4(4):307-20.

38.    Johnstone TC, Suntharalingam K, Lippard SJ. The Next Generation of Platinum Drugs: Targeted Pt (II) Agents, Nanoparticle Delivery, and Pt (IV) Prodrugs. Chem Rev. 2016;116(5):3436-86.

39.    Kelland L. The resurgence of platinum-based cancer chemotherapy. Nat Rev Cancer. 2007;7(8):573-84.

40.     Yu F, Megyesi J, Safirstein RL, et al. Involvement of the CDK2-E2F1 pathway in cisplatin cytotoxicity in *vitro* and in *vivo*. Am J Physiol Renal Physiol. 2007;293(1):F52-9.

41.     Xu Y, Wang C, Li Z. A new strategy of promoting cisplatin chemotherapeutic efficiency by targeting endoplasmic reticulum stress. Mol Clin Oncol. 2014;2(1):3-7.

42.     Rodriguez D, Rojas-Rivera D, Hetz C. Integrating stress signals at the endoplasmic reticulum: The BCL-2 protein family rheostat. Biochim Biophys Acta. 2011;1813(4):564-74.

43.     Rashid HO, Yadav RK, Kim HR, Chae HJ. ER stress: Autophagy induction, inhibition and selection. Autophagy. 2015;11(11):1956-77.

44.     Xu Y, Yu H, Qin H, et al. Inhibition of autophagy enhances cisplatin cytotoxicity through endoplasmic reticulum stress in human cervical cancer cells. Cancer Lett. 2012;314(2):232-43.

45.     Hetz C, Chevet E, Oakes SA. Proteostasis control by the unfolded protein response. Nat. Cell Biol. 2015;17(8):829-38.

46.     Chevet E, Hetz C, Samali A. Endoplasmic reticulum stress-activated cell reprogramming in oncogenesis. Cancer Discov. 2015;5(6):586-97.

47.     Dejeans N, Barroso K, Fernandez-Zapico ME, et al. Novel roles of the unfolded protein response in the control of tumor development and aggressiveness. Semin Cancer Biol. 2015;33:67-73.

48.     Schubert U, Anton LC, Gibbs J, et al. Rapid degradation of a large fraction of newly synthesized proteins by proteasomes. Nature. 2000;404(6779):770-4.

49.     Hetz C, Chevet E, Oakes SA. Erratum: Proteostasis control by the unfolded protein response. Nat Cell Biol. 2015;17(8):1088.

50.     da Silva DC, Valentao P, Andrade PB, et al. Endoplasmic reticulum stress signaling in cancer and neurodegenerative disorders: tools and strategies to understand its complexity.Pharmacol Res. 2020 : 104702.

51.     Romero-Ramirez L, Cao H, Nelson D, et al. *XBP1* is essential for survival under hypoxic conditions and is required for tumor growth. Cancer Res. 2004;64(17):5943-7.

52.     Jamora C, Dennert G, Lee AS. Inhibition of tumor progression by suppression of stress protein GRP78/BiP induction in fibrosarcoma B/C10ME. Proc Natl Acad Sci U S A. 1996;93(15):7690-4.

53.     Bi M, Naczki C, Koritzinsky M, et al. ER stress-regulated translation increases tolerance to extreme hypoxia and promotes tumor growth. EMBO J. 2005;24(19):3470-81.

54.     Wang M, Kaufman RJ. The impact of the endoplasmic reticulum protein-folding environment on cancer development. Nat Rev Cancer. 2014;14(9):581-97.

55.     Urra H, Dufey E, Lisbona F, Rojas-Rivera D, Hetz C, et al. When ER stress reaches a dead end. Biochim Biophys Acta. 2013;1833(12):3507-17.

56.     Clarke R, Cook KL, Hu R, et al. Endoplasmic reticulum stress, the unfolded protein response, autophagy, and the integrated regulation of breast cancer cell fate. Cancer Res. 2012;72(6):1321-31.

57.     Haze K, Yoshida H, Yanagi H, et al. Mammalian transcription factor ATF6 is synthesized as a transmembrane protein and activated by proteolysis in response to endoplasmic reticulum stress. Mol Biol Cell. 1999;10(11):3787-99.

58.     Tirasophon W, Welihinda AA, Kaufman RJ. A stress response pathway from the endoplasmic reticulum to the nucleus requires a novel bifunctional protein

kinase/endoribonuclease (Ire1p) in mammalian cells. Genes Dev. 1998;12(12):1812-24.

59.     Harding HP, Zhang Y, Ron D. Protein translation and folding are coupled by an endoplasmic-reticulum-resident kinase. Nature. 1999;397(6716):271-4.

60.     Smith JA. A new paradigm: innate immune sensing of viruses via the unfolded protein response. Frontiers in Microbiology. 2014;5(222).

61.     Hetz C, Chevet E, Oakes SA. Proteostasis control by the unfolded protein response. Nat Cell Biol. 2015;17(7):829-38.

62.     Carrara M, Prischi F, Nowak PR, et al. Noncanonical binding of BiP ATPase domain to IRE1 and PERK is dissociated by unfolded protein CH1 to initiate ER stress signaling. Elife. 2015;4: e03522.

63.     Bertolotti A, Zhang Y, Hendershot LM, et al. Dynamic interaction of BiP and ER stress transducers in the unfolded-protein response. Nat Cell Biol. 2000;2(6):326-32.

64.     Nadanaka S, Okada T, Yoshida H, et al. Role of disulfide bridges formed in the luminal domain of ATF6 in sensing endoplasmic reticulum stress. Mol Cell Biol. 2007;27(3):1027-43.

65.     Shen J, Chen X, Hendershot L, et al. ER stress regulation of ATF6 localization by dissociation of BiP/GRP78 binding and unmasking of Golgi localization signals. Dev Cell. 2002;3(1):99-111.

66.     Sun H, Lin DC, Guo X, et al. Inhibition of IRE1alpha-driven pro-survival pathways is a promising therapeutic application in acute myeloid leukemia. Oncotarget. 2016;7(14):18736-49.

67.     Lee AH, Glimcher LH. Intersection of the unfolded protein response and hepatic lipid metabolism. Cell Mol Life Sci. 2009;66(17):2835-50.

68.     Chen Y, Brandizzi F. IRE1: ER stress sensor and cell fate executor. Trends Cell Biol. 2013;23(11):547-55.

69.     Clarke HJ, Chambers JE, Liniker E, et al. Endoplasmic reticulum stress in malignancy. Cancer Cell. 2014;25(5):563-73.

70.     Binet F, Sapieha P. ER Stress and Angiogenesis. Cell Metab. 2015;22(4):560-75.

71.     Nishitoh H, Matsuzawa A, Tobiume K, et al. ASK1 is essential for endoplasmic reticulum stress-induced neuronal cell death triggered by expanded polyglutamine repeats. Genes Dev. 2002;16(11):1345-55.

72.     DuRose JB, Scheuner D, Kaufman RJ, et al. Phosphorylation of eukaryotic translation initiation factor 2alpha coordinates rRNA transcription and translation inhibition during endoplasmic reticulum stress. Mol Cell Biol. 2009;29(15):4295-307.

73.     Rozpedek W, Pytel D, Mucha B, et al. The role of the PERK/eIF2alpha/ATF4/CHOP signaling pathway in tumor progression during endoplasmic reticulum stress. Curr Mol Med. 2016;16(6):533-44.

74.     Cabrera E, Hernandez-Perez S, Koundrioukoff S, et al. PERK inhibits DNA replication during the unfolded protein response via claspin and Chk1. Oncogene. 2017;36(5):678-86.

75.     McQuiston A, Diehl JA. Recent insights into PERK-dependent signaling from the stressed endoplasmic reticulum. F1000Res. 2017;6:1897.

76.     Yamamoto K, Sato T, Matsui T, et al. Transcriptional induction of mammalian ER quality control proteins is mediated by single or combined action of ATF6 α and *XBP1*. Dev Cell. 2007;13(3):365-76.

77.     Yoshida H, Matsui T, Yamamoto A, et al. *XBP1* mRNA is induced by ATF6 and spliced by IRE1 in response to ER stress to produce a highly active transcription factor. Cell. 2001;107(7):881-91.

78.     Chen X, Guo X, Ge Q, et al. ER stress activates the NLRP3 Inflammasome: A novel mechanism of atherosclerosis. Ocid. Med. Cell. Longev. 2019;2019:3462530.

79.     Acosta-Alvear D, Zhou Y, Blais A, et al. *XBP1* controls diverse cell type- and condition-specific transcriptional regulatory networks. Mol Cell. 2007;27(1):53-66.

80.     Papandreou I, Denko NC, Olson M, et al. Identification of an Ire1 α endonuclease specific inhibitor with cytotoxic activity against human multiple myeloma. Blood. 2011;117(4):1311-4.

81.     Matsukawa J, Matsuzawa A, Takeda K, et al. The ASK1-MAP kinase cascades in mammalian stress response. J Biochem. 2004;136(3):261-5.

82.     Fischer H, Koenig U, Eckhart L, et al. Human caspase 12 has acquired deleterious mutations. Biochem Biophys Res Commun. 2002;293(2):722-6.

83.     Dhanasekaran DN, Reddy EP. JNK signaling in apoptosis. Oncogene. 2008;27(48):6245-51.

84.     Harris CA, Johnson EM, Jr. BH3-only Bcl-2 family members are coordinately regulated by the JNK pathway and require Bax to induce apoptosis in neurons. J Biol Chem. 2001;276(41):37754-60.

85.     Sehgal V, Ram PT. Network Motifs in JNK Signaling. Genes Cancer. 2013;4(9-10):409-13.

86.     Barr RK, Bogoyevitch MA. The c-Jun N-terminal protein kinase family of mitogen-activated protein kinases (JNK MAPKs). Int J Biochem Cell Biol. 2001;33(11):1047-63.

87.     Tournier C, Dong C, Turner TK, et al. MKK7 is an essential component of the JNK signal transduction pathway activated by proinflammatory cytokines. Genes Dev. 2001;15(11):1419-26.

88.     Haeusgen W, Herdegen T, Waetzig V. The bottleneck of JNK signaling: molecular and functional characteristics of MKK4 and MKK7. Eur J Cell Biol. 2011;90(6-7):536-44.

89.     Besirli CG, Johnson EM, Jr. JNK-independent activation of c-Jun during neuronal apoptosis induced by multiple DNA-damaging agents. J Biol Chem. 2003;278(25):22357-66.

90.     Huntwork-Rodriguez S, Wang B, Watkins T, et al. JNK-mediated phosphorylation of DLK suppresses its ubiquitination to promote neuronal apoptosis. J Cell Biol. 2013;202(5):747-63.

91.     Ambacher KK, Pitzul KB, Karajgikar M, et al. The JNK- and AKT/GSK3β-signaling pathways converge to regulate Puma induction and neuronal apoptosis induced by trophic factor deprivation. PloS one. 2012;7(10):e46885-e.

92.     Yuan Z, Wang F, Zhao Z, et al. BIM-mediated AKT phosphorylation is a key modulator of arsenic trioxide-induced apoptosis in cisplatin-sensitive and -resistant ovarian cancer cells. PloS one. 2011;6(5):e20586.

93.     Yu J, Zhang L. PUMA, a potent killer with or without p53. Oncogene. 2008;27(1):S71-S83.

94.     Ebada SS, Edrada RA, Lin W, et al. Methods for isolation, purification and structural elucidation of bioactive secondary metabolites from marine invertebrates. Nat Protoc. 2008;3(12):1820-31.

95.     Kanz C, Aldebert P, Althorpe N, et al. The EMBL nucleotide sequence database. Nucleic Acids Res. 2005;33(Database issue):D29-33.

96.     Kinghorn AD, Chin Y-W, Swanson SM. Discovery of natural product anticancer agents from biodiverse organisms. Curr Opin Drug Discov Devel. 2009;12(2):189-96.

97.     Williams ST, Goodfellow M, Alderson G, et al. Numerical classification of Streptomyces and related genera. J Gen Microbiol. 1983;129(6):1743-813.

98.     Williams ST, Goodfellow M, Wellington EM, et al. A probability matrix for identification of some Streptomycetes. J Gen Microbiol. 1983;129(6):1815-30.

99.     Srinivasan MC, Laxman RS, Deshpande MV. Physiology and nutritional aspects of actinomycetes: an overview. World J Microbiol Biotechnol. 1991;7(2):171-84.

100.    Chamikara P. Actinomycetes. 2016.

101.    Posa MRC, Wijedasa LS, Corlett RT. Biodiversity and Conservation of Tropical Peat Swamp Forests. BioScience. 2011;61(1):49-57.

102.    Tolsma AD. The Biology of Peatlands, 2nd edition by H. Rydin and J. K. Jeglum. Oxford University Press, Oxford, 2013. Austral Ecol. 2015;40(8):e18-e9.

103.    Rubec C. The canadian wetland classification system. The wetland book: I: structure and function, management, and methods. Dordrecht: Springer Netherlands; 2018. p. 1577-81.

104. Janda JM, Abbott SL. 16S rRNA gene sequencing for bacterial identification in the diagnostic laboratory: pluses, perils, and pitfalls. J Clin Microbiol. 2007;45(9):2761-4.

105. Clarridge JE, 3rd. Impact of 16S rRNA gene sequence analysis for identification of bacteria on clinical microbiology and infectious diseases. Clin Microbiol Rev. 2004;17(4):840-62.

106. Petti CA. Detection and identification of microorganisms by gene amplification and sequencing. Clin Infect Dis. 2007;44(8):1108-14.

107. Huson DH, Richter DC, Mitra S, et al. Methods for comparative metagenomics. BMC Bioinformatics. 2009;10(1):S12.

108. Balloux F, Brønstad Brynildsrud O, van Dorp L, et al. From theory to practice: translating whole-genome sequencing (WGS) into the clinic. Trends Microbiol. 2018;26(12):1035-48.

109. Blin K, Shaw S, Steinke K, Villebro R, Ziemert N, Lee SY, et al. antiSMASH 5.0: updates to the secondary metabolite genome mining pipeline. Nucleic Acids Res. 2019;47(W1):W81-W7.

110. reza Dehnad A, Yeganeh LP, Bakhshi R, et al. Investigation antibacterial activity of Streptomycetes isolates from soil samples, West of Iran. Afr. J. Microbiol. Res. 2010;4(16):1685-93.

111. Kavitha A, Vijayalakshmi M, Sudhakar P, et al. Screening of actinomycetes strains for the production of antifungal metabolites. Afr. J. Microbiol. Res. 2010;4(1):027-32.

112.    Willemse J, Borst JW, de Waal E, et al. Positive control of cell division: FtsZ is recruited by SsgB during sporulation of *Streptomyces*. Genes Dev. 2011;25(1):89-99.

113.    Chater KF. Genetics of differentiation in *Streptomyces*. Annu Rev Microbiol. 1993;47:685-713.

114.    Jüttner F, Watson SB. Biochemical and Ecological Control of Geosmin and 2-Methylisoborneol in Source Waters. Applied and Environmental Microbiology. 2007;73(14):4395.

115.    Ambarwati A, Sembiring L, Soegihardjo C. Antibiotic produced by streptomycetes associated with rhizosphere of purple nut sedge (*Cyperus rotundus L.*) in Surakarta, Indonesia. Afr. J. Microbiol. Res. 2012;6(1):52-7.

116.    Flärdh K, Buttner MJ. *Streptomyces* morphogenetics: dissecting differentiation in a filamentous bacterium. Nat. Rev. Microbiol. 2009;7(1):36-49.

117.    James PD, Edwards C. The effects of temperature on growth and production of the antibiotic granaticin by a thermotolerant streptomycete. J Gen Microbiol. 1989;135(7):1997-2003.

118.    Basilio A, González I, Vicente MF, et al. Patterns of antimicrobial activities from soil actinomycetes isolated under different conditions of pH and salinity. J Appl Microbiol. 2003;95(4):814-23.

119.    Mcgregor JF. Nuclear Division and the Life Cycle in a *Streptomyces* sp. Microbiology. 1954;11(1):52-6.

120.    Horinouchi S. A microbial hormone, A-factor, as a master switch for morphological differentiation and secondary metabolism in *Streptomyces griseus*. Front Biosci. 2002;7:d2045-57.

121.    Hwang KS, Kim HU, Charusanti P, et al. Systems biology and biotechnology of *Streptomyces* species for the production of secondary metabolites. Biotechnol Adv. 2014;32(2):255-68.

122.    Worrall JA, Vijgenboom E. Copper mining in *Streptomyces*: enzymes, natural products and development. Nat Prod Rep. 2010;27(5):742-56.

123.    Demain AL. Microbial production of primary metabolites. Sci. Nat.. Die. 1980;67(12):582-7.

124.    Shomura T, Yoshida J, Amano S, et al. Studies on Actinomycetales producing antibiotics only on agar culture. I. Screening, taxonomy and morphology-productivity relationship of *Streptomyces halstedii*, strain SF-1993. J Antibiot (Tokyo). 1979;32(5):427-35.

125.    Drew SW, Demain AL. Effect of primary metabolites on secondary metabolism. Annu Rev Microbiol. 1977;31:343-56.

126.    Boubetra D, Sabaou N, Zitouni A, et al. Taxonomy and chemical characterization of new antibiotics produced by *Saccharothrix* SA198 isolated from a Saharan soil. Microbiological research. 2012;168.

127.    Mukhtar H. Production of antitumor antibiotic by *streptomyces capoamus*. Pak. J.Bot. 2012;44:445-52.

128.    Cheng YR, Fang A, Demain AL. Effect of amino acids on rapamycin biosynthesis by *Streptomyces hygroscopicus*. Appl Microbiol Biotechnol. 1995;43(6):1096-8.

129.    Demain AL, Sanchez S. Microbial drug discovery: 80 years of progress. **J**. Antibiot. 2009;62(1):5-16.

130. Arcamone F, Cassinelli G, Fantini G, et al. Adriamycin, 14-hydroxydaunomycin, a new antitumor antibiotic from *S. peucetius* var. caesius. Biotechnol Bioeng. 2000;67(6):704-13.

131. Wang Z, Gleichmann H. GLUT2 in pancreatic islets: crucial target molecule in diabetes induced with multiple low doses of streptozotocin in mice. Diabetes. 1998;47(1):50-6.

132. Wu CZ, Jang JH, Ahn JS, et al. New geldanamycin analogs from *Streptomyces hygroscopicus*. J Microbiol Biotechnol. 2012;22(11):1478-81.

133. Gorajana A, Venkatesan M, Vinjamuri S, et al. Resistoflavine, cytotoxic compound from a marine actinomycete, *Streptomyces chibaensis* AUBN1/7. Microbiol Res. 2007;162(4):322-7.

134. Bhatnagar I, Kim SK. Immense essence of excellence: marine microbial bioactive compounds. Mar Drugs. 2010;8(10):2673-701.

135. Hawas UW, Shaaban M, Shaaban KA, et al. Mansouramycins A-D, cytotoxic isoquinolinequinones from a marine *streptomycete*. J Nat Prod. 2009;72(12):2120-4.

136. Montaser R, Luesch H. Marine natural products: a new wave of drugs? Future Med Chem. 2011;3(12):1475-89.

137. Pérez M, Crespo C, Schleissner C, et al. Tartrolon D, a cytotoxic macrodiolide from the marine-derived actinomycete *Streptomyces* sp. MDG-04-17-069. J. Nat. Prod. 2009;72(12):2192-4.

138. Waksman SA, Woodruff HB. Actinomyces antibioticus, a new soil organism antagonistic to pathogenic and non-pathogenic bacteria. J Bacteriol. 1941;42(2):231-49.

139. Hohmann C, Schneider K, Bruntner C, et al. Caboxamycin, a new antibiotic of the benzoxazole family produced by the deep-sea strain *Streptomyces* sp. NTK 937. J Antibiot (Tokyo). 2009;62(2):99-104.

140. Zhou W, Fang H, Wu Q, et al. Ilamycin E, a natural product of marine actinomycete, inhibits triple-negative breast cancer partially through ER stress-CHOP-Bcl-2. Int J Biol Sci. 2019;15(8):1723-32.

141. Futamura Y, Tashiro E, Hironiwa N, et al. Trierixin, a novel Inhibitor of ER stress-induced *XBP1* activation from *Streptomyces* sp. II. structure elucidation. J Antibiot (Tokyo). 2007;60(9):582-5.

142. Wattam AR, Abraham D, Dalay O, et al. PATRIC, the bacterial bioinformatics database and analysis resource. Nucleic Acids Res. 2014;42(Database issue):D581-91.

143. Meier-Kolthoff JP, Göker M. TYGS is an automated high-throughput platform for state-of-the-art genome-based taxonomy. Nat. Commun. 2019;10(1):2182.

144. Richter M, Rosselló-Móra R, Oliver Glöckner F, et al. JSpeciesWS: a web server for prokaryotic species circumscription based on pairwise genome comparison. Bioinformatics. 2016;32(6):929-31.

145. Blin K, Shaw S, Steinke K, et al. antiSMASH 5.0: updates to the secondary metabolite genome mining pipeline. Nucleic Acids Res. 2019;47(W1):W81-w7.

146. Pinkaew D, Chattopadhyay A, King MD, et al. Fortilin binds IRE1 α and prevents ER stress from signaling apoptotic cell death. Nat Commun. 2017;8(1):18.

147. Wayne LG, Brenner DJ, Colwell RR, et al. Report of the Ad Hoc committee on reconciliation of approaches to bacterial systematics. Int. J. Syst. Evol. 1987;37(4):463-4.

148. Richter M, Rosselló-Móra R. Shifting the genomic gold standard for the prokaryotic species definition. Proc Natl Acad Sci U S A. 2009;106(45):19126-31.

149. Gürtler H, Pedersen R, Anthoni U, et al. Albaflavenone, a sesquiterpene ketone with a zizaene skeleton produced by a streptomycete with a new rope morphology. J Antibiot (Tokyo). 1994;47(4):434-9.

150. Leary M, Heerboth S, Lapinska K, et al. Sensitization of drug resistant cancer cells: A matter of combination therapy. Cancers (Basel). 2018;10(12).

151. Ayuso A, Clark D, González I, et al. A novel actinomycete strain de-replication approach based on the diversity of polyketide synthase and nonribosomal peptide synthetase biosynthetic pathways. Appl. Microbiol. Biotechnal. 2005;67(6):795-806.

152. Rieger AM, Nelson KL, Konowalchuk JD, et al. Modified annexin V/propidium iodide apoptosis assay for accurate assessment of cell death. J Vis Exp. 2011(50):2597.

153. Ventura JJ, Hübner A, Zhang C, et al. Chemical genetic analysis of the time course of signal transduction by JNK. Mol Cell. 2006;21(5):701-10.

154. Dan VM, Muralikrishnan B, Sanawar R, et al. *Streptomyces* sp. metabolite(s) promotes Bax mediated intrinsic apoptosis and autophagy involving inhibition of mTOR pathway in cervical cancer cell lines. Sci. Rep. 2018;8(1):2810.

155. Liu L, Zhu H, Wu W, et al. Neoantimycin F, a *Streptomyces*-derived natural product induces mitochondria-related apoptotic death in human non-small cell lung cancer cells. Front Pharmacol. 2019;10:1042-.

# APPENDICES

## APPENDIX A

### 1.Genomic study of *Streptomyces* sp. ST1-45

An assembled genome of *Streptomyces* sp. ST1-45 was submitted to the comprehensive genome analysis service using PATRIC. Based on the analysis of PATRIC pipeline, the genome provided good quality. This assembled genome included 222 contigs with a length of 8,937,732 bp and the average G+C content was 71.08%. This genome has 8,716 protein-coding sequence (CDS), 68 transfer RNA (tRNA) genes, and 5 ribosomal RNA (rRNA) genes. These ribosomal RNA genes contained two 23S rRNA genes, two 16S rRNA gene, and one 5S rRNA. The genome annotation consisted of 3075 hypothetical proteins, 5,641 protein with functional assignment, 1237 with Gene Ontology (GO) assignments.

The graphical display of circular view of the genome was shown in Fig.17. The result included, from the outer to inner rings, the contigs, CDS on the forward strand, CDS on the reverse strand, non-CDS feature, antimicrobial resistance genes, virulence factor genes, transporters, drug targets, GC content, and GC skew. The color of the CDS on the forward and reverse strand represents the subsystem that this gene belongs to (Fig.18).
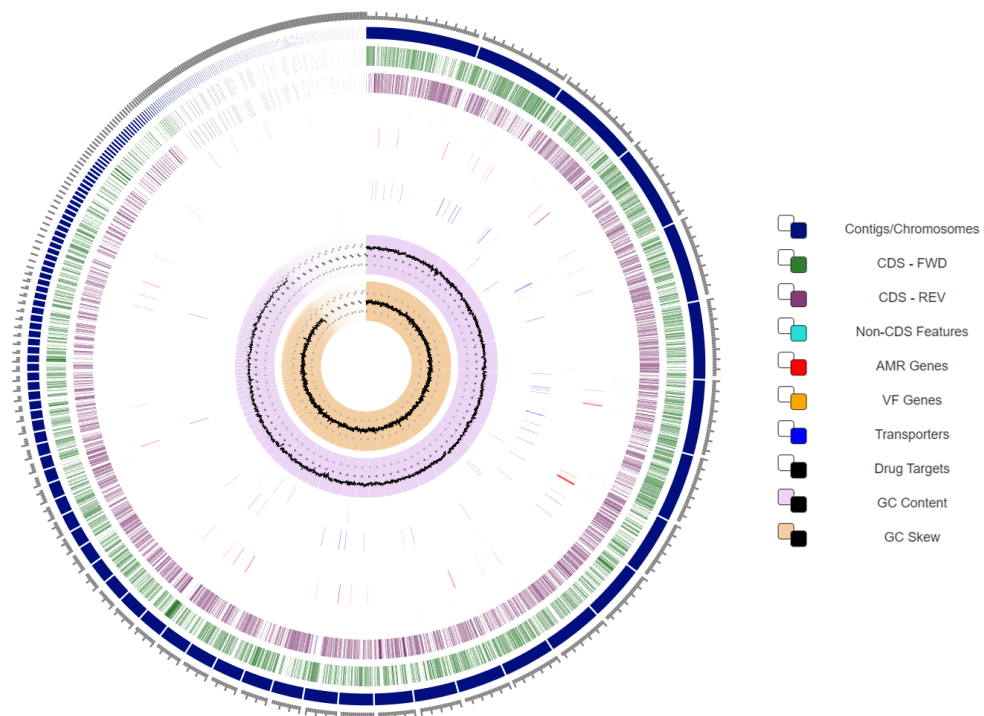
**Figure 18** The circular view of the genome of Streptomyces strain ST1-45.



**Subsystem Counts** (Subsystems, Genes)
> METABOLISM (100, 969)
> ENERGY (29, 368)
> PROTEIN PROCESSING (41, 291)
> STRESS RESPONSE, DEFENSE, VIRULENCE (34, 182)
> CELLULAR PROCESSES (14, 127)
> DNA PROCESSING (17, 104)
> REGULATION AND CELL SIGNALING (6, 69)
> MEMBRANE TRANSPORT (9, 50)
> RNA PROCESSING (10, 49)
> CELL ENVELOPE (6, 23)
> MISCELLANEOUS (4, 15)
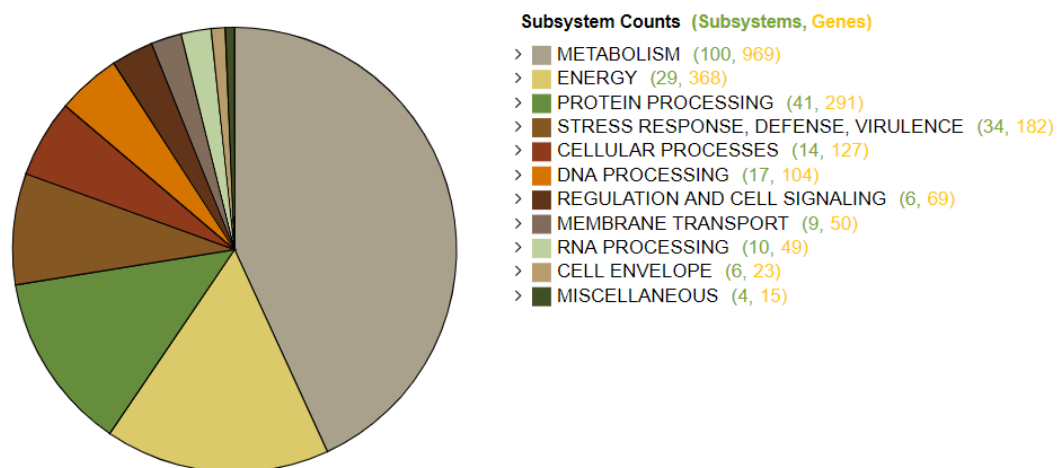
**Figure 19** The overview of the genome of the subsystems of the strain ST1-45. The subsystem provides a set of proteins that together implement a specific biological process or structural complex.

**Table 5** Results of 16S rRNA gene analysis

| No. | Isolates | Strain | Similarity | Accession Number |
|-----|----------|--------|------------|------------------|
| 1. | ST1-45 | *Streptomyces fodineus* TW1S1$^T$ | 98.48 % | KT820007 |
| 2. | ST1-64 | *Streptomyces lucensis* NBRC13056$^T$ | 99.20 % | AB184280 |
| 3. | ST1-54 | *Streptomyces glomeratus* LMG19903$^T$ | 99.53 % | AJ781754 |
| 4. | ST1-39 | *Streptomyces stelliscabiei* NRRLB-2447$^T$ | 98.80 % | FJ007385 |
| 5. | ST1-69 | Ochrobactum intermedium LMG3301$^T$ | 99.85 % | AB680967 |
| 6. | ST1-63 | Ochrobactum intermedium LMG3301$^T$ | 99.80 % | AB680967 |
| 7. | ST1-29 | Ochrobactum intermedium LMG3301$^T$ | 99.62 % | AB680967 |
| 8. | ST1-42 | *Streptomyces fodineus* TW1S1$^T$ | 99.15 % | KT820007 |

## APPENDIX B

## PREPARATION OF REAGENTS

**Yeast extract-malt extract agar (ISP medium 2, ISP 2)**

| | |
|---|---|
| Bacto-Yeast Extract (Difco) | 4 g |
| Bacato-Malt Extract (Difco) | 10 g |
| Bacto-Dextrose (Glucose) | 4 g |
| Distilled Water | 1 L |
| Adjust to pH- (7 to 7.2), then add | |
| Bacto agar | 16 g |

**301 Seed medium**

| | |
|---|---|
| Starch (2.4 %) | 24 g |
| Glucose Extract (0.1%) | 1 g |
| Peptone Extract (0.3%) | 3 g |
| Meat Extract (0.3%) | 3 g |
| Yeast Extract (0.5%) | 3 g |
| $CaCO_3$ (0.4%) | 5 g |
| Distilled Water | 1 L |
| pH - 7.00 | |

**TE buffer**

| | |
|---|---|
| 10 mM Tris-HCl (pH 8.0) | 10 mL |
| 1 mM Na2-EDTA (pH 8.0) | 10 mL |
| Distilled water | 980 mL |

**1 M Tris-HCl buffer, pH 8.0**

       Tris base           121.1 mg

  Dissolve Tris base in distilled water. Stir solution and monitor the pH with a

pH probe while adding conc. HCl to adjust the pH 8.0. Make up the solution to 1 L

with distilled water and autoclave. Store it at room temperature.

**1 mM Na2-EDTA (pH 8.0)**

       EDTA          292.24 g

Dissolve EDTA in 700 ml of distilled water. Stir solution and monitor the pH with a

pH probe while adding NaOH pellets to adjust the pH 8.0. Dilute the solution to 1 l

with distilled water and autoclave. Store it at room temperature.

**3 M Sodium acetate**

  Sodium acetate trihydrate (CH3COONa.3H2O)   408.0 g

 Dissolve CH3COONa.3H2O in 400 ml of distilled water. Stir solution and monitor

the pH with a pH probe while adding glacial acetic acid to adjust the pH 5.2. Make up

the solution to 1 L with distilled water and autoclave.

**50X Tris-acetate (TAE) buffer**

  Tris Base           242.28 g

  Glacial acetic acid        57.1 mL

  0.5M EDTA (pH 8.0)      100 mL

Dissolve Tris Base in 600 ml of distilled water. Stir solution and add glacial acetic

acid and 0.5M EDTA (pH 8.0) solution. Make up the volume to 1000 ml with distilled

water. Autoclave and store at room temperature.

**1X Tris-acetate (TAE) buffer**

| | |
|---|---|
| 50X Tris-acetate (TAE) buffer | 20 mL |
| Distilled water | 980 mL |

**0.8% Agarose gel**

| | |
|---|---|
| Agarose | 0.8 g |
| Distilled water | 100 mL |

Mix agarose and distilled water and melt the mixture with the microwave.

**2% Agarose gel**

| | |
|---|---|
| Agarose | 0.8 g |
| Distilled water | 100 mL |

Mix agarose and distilled water and melt the mixture with the microwave.

**Lysozyme digestion buffer (20 mg/mL)**

| | |
|---|---|
| Lysozyme | 10 mg |
| TE buffer | 500 μL |

**10 X Running Buffer (pH- 8.3)**

| | |
|---|---|
| 250 mM Tris Base | 30.3 g |
| 1.92 M Glycine | 144 g |
| 1% SDS | 10 g |
| Distilled water | 1 L |

**1 X Running Buffer**

| 10X Running Buffer | 100 mL |
| Distilled water | 900 mL |

**1 X Transfer Buffer**

| 48 mM Tribase | 5.815 g |
| 39 mM Glycine | 2.925 g |
| 20% Methanol | 200 mL |
| 0.04% SDS | 0.4 g |
| Distilled water | 1 L |

**10X TBS (pH- 7.6)**

| Tri-base | 24.23 g |
| NaCL | 80.06 g |
| Distilled water | 1 L |

**1X TBST**

| 10X TBS | 100 mL |
| Distilled water | 900 mL |

**Anisaldehyde reagent**

| Ethanol | 90 mL |
| Conc: $H_2SO_4$ | 5 mL |
| p-Anisaldegyde | 5 mL |
| Acetic acid | 1 mL |

**Dragendorff's reagent**

Solution A

| | |
|---|---|
| Basic bismuth nitrate | 1.7 g |
| Acetic acid | 20 ml |
| Distilled water | 80 ml |

Solution B

| | |
|---|---|
| KI | 40 g |
| Distilled water | 100 ml |

Before spraying, 10 mL of each solution A plus solution B and acetic acid (10 ml).

**Ninhydrin**

| | |
|---|---|
| Ninhydrin | 0.2 g |
| Absolute alcohol | 100 mL |

**Phosphomolybdic acid reagent**

| | |
|---|---|
| Absolute ethanol | 100 ml |
| Phosphomolybdic acid | 5.0 g |

**Sulfuric acid (H2SO4/LWUV)**

| | |
|---|---|
| Concentrated sulfuric acid | 100 mL |
| Distilled water | 100 mL |

**Sulfuric acid/Methanol/LWUV**

| | |
|---|---|
| Concentrated sulfuric acid | 10 mL |
| Methanol | 90 mL |

# APPENDIX C

## TABLES OF EXPERIMENTAL RESULTS

**Table 6** The percentage of cell viability of human H460 lung cancer cell after treatment with 0-160 µg/mL of *Streptomyces* crude extract (ST1-45).

| ST1-45 (µg/mL) | % Cell Viability |
|---|---|
| - | $100.00 \pm 0.00$ |
| 0.625 µg/mL | $90.77 \pm 5.36$ |
| 2.5 µg/mL | $71.58 \pm 9.69*$ |
| 10 µg/mL | $50.69 \pm 10.05*$ |
| 40 µg/mL | $46.96 \pm 9.17*$ |
| 160 µg/mL | $34.16 \pm 9.17*$ |

Values are average from five independent experiments $\pm$ SD.

*$P \leq 0.05$ versus non-treated control.

**Table 7** The percentage of cell viability of human H460 lung cancer cell after treatment with 0-160 µg/mL of *Streptomyces* crude extract (ST1-64).

| ST1-64 (µg/mL) | % Cell Viability |
|---|---|
| - | 100.00 ± 0.00 |
| 0.625 µg/mL | 95.21 ± 0.56 |
| 2.5 µg/mL | 89.16 ± 3.48 |
| 10 µg/mL | 87.45 ± 4.64* |
| 40 µg/mL | 81.30 ± 6.72* |
| 160 µg/mL | 74.00 ± 9.29* |

Values are average from five independent experiments ± SD.

*$P \leq 0.05$ versus non-treated control.

**Table 8** The percentage of cell viability of human H460 lung cancer cell after treatment with 0-160 µg/mL of *Streptomyces* crude extract (ST1-54).

| ST1-54 (µg/mL) | % Cell Viability |
|---|---|
| - | 100.00 ± 0.00 |
| 0.625 µg/mL | 95.86 ± 3.94 |
| 2.5 µg/mL | 92.67 ± 4.77 |
| 10 µg/mL | 86.34 ± 2.63* |
| 40 µg/mL | 74.64 ± 4.39* |
| 160 µg/mL | 55.23 ± 9.40* |

Values are average from five independent experiments ± SD.

*$P \leq 0.05$ versus non-treated control.

**Table 9** The percentage of cell viability of human H460 lung cancer cell and non-cancerous human keratinocyte cell (HaCaT) after treatment with 0-5 µg/mL of *Streptomyces* crude extract (ST1-45).

| ST1-45 (µg/mL) | % Cell Viability | |
| --- | --- | --- |
| | H460 | HaCaT |
| - | $100.00 \pm 0.00$ | $100.00 \pm 0.00$ |
| 0.3 µg/mL | $98.75 \pm 0.37$ | $94.58 \pm 1.60$ |
| 0.625 µg/mL | $95.23 \pm 4.06$ | $92.97 \pm 0.20$ |
| 1.25 µg/mL | $91.32 \pm 4.31$ | $92.50 \pm 0.14$ |
| 2.5 µg/mL | $83.19 \pm 3.73*$ | $91.60 \pm 0.34$ |
| 5 µg/mL | $64.97 \pm 3.64*$ | $90.55 \pm 0.36$ |

Values are average from five independent experiments ± SD.

*$P \leq 0.05$ versus non-treated control.

**Table 10** The percentage of cell viability of human H460 lung cancer cell after treatment with 1.25 µg/mL of *Streptomyces* crude extract (ST1-45) for 1 h followed by 0-40 µM of cisplatin.

| Cisplatin (µM) | % Cell Viability | |
| --- | --- | --- |
| | Cotreatment | Cisplatin aone |
| - | 100.00 ± 0.00 | 100.00 ± 0.00 |
| 2.5 µM | 56.53 ± 4.64*# | 96.67 ± 3.35 |
| 5 µM | 52.57 ± 6.48*# | 95.52 ± 3.14 |
| 10 µM | 46.14 ± 4.46*# | 93.85 ± 4.87 |
| 20 µM | 32.51 ± 0.48*# | 85.33 ± 4.19 |
| 40 µM | 18.83 ± 6.46*# | 40.79 ± 4.43* |

Values are average from five independent experiments ± SD.

*$P \leq 0.05$ versus non-treated control.

#$P \leq 0.05$ versus the cells treated with cisplatin alone.

**Table 11** The relative protein expression level of ER stress markers after pretreated
with ST1-45 for 1 h followed by various concentrations of cisplatin on
human H460 lung cancer cells.

| Treatment groups | Relative protein level | | |
|---|---|---|---|
| | pIRE1 α | pJNK | JNK |
| Control | 1.00±0.00 | 1.00±0.00 | 1.00±0.00 |
| ST1-45 | 0.94±0.39 | 2.62±0.43 | 0.96±0.13 |
| Cisplatin 2.5 | 0.93±0.36 | 1.6±0.22 | 0.98±0.35 |
| ST1-45 + Cisplatin 2.5 | 0.89±0.78 | 1.30±0.53 | 0.91±0.23 |
| Cisplatin 5 | 0.90±0.90 | 1.34±0.23 | 0.89±0.31 |
| ST1-45 + Cisplatin 5 | 0.85±0.86 | 1.37±0.31 | 0.88±0.46 |
| Cisplatin 10 | 0.98±0.89 | 1.25±0.25 | 0.80±0.44 |
| ST1-45 + Cisplatin 10 | 0.80±0.54 | 3.25±0.44 | 0.92±0.24 |

Values are average from five independent experiments ± SD.

*$P \leq 0.05$ versus non-treated control.

# VITA

| | |
|---|---|
| **NAME** | Theint Myat Noe Paing |
| **DATE OF BIRTH** | 12 November 1993 |
| **PLACE OF BIRTH** | Myanmar |
| **INSTITUTIONS ATTENDED** | University of Pharmacy (Ygn) |
| **HOME ADDRESS** | No (106), Thamasateta Street, Nyaung Lay Pin Township, Pago Division, Myanmar. |